JOURNAL OF GEOPHYSICAL RESEARCH, VOL. 112, E06005, doi:10.1029/2006JE002787, 2007

Combinations of processes responsible for Martian impact crater "layered ejecta structures" emplacement

Goro Komatsu,[1] Gian Gabriele Ori,[1] Stefano Di Lorenzo,[1] Angelo Pio Rossi,[1,2] and Gerhard Neukum[3]

Received 3 July 2006; revised 20 October 2006; accepted 24 January 2007; published 16 June 2007.

[1] We utilized images and stereo-derived topographic data acquired by the High Resolution Stereo Camera (HRSC) and Thermal Emission Imaging System (THEMIS) images together with other data in order to study the geology of ''layered ejecta structures'' associated with relatively pristine Martian impact craters. The geomorphology and morphometric properties indicate their origin as complex combinations of a variety of impact processes. The studied (inner) layered ejecta structures often exhibit ground-hugging characteristics, and many of them do not have topographic profiles expected from simple ballistic emplacement. Such profiles include ones that are plateau-shaped or thickening outward. We think that water-rich fluidized flows driven by the momentum due to the impact and by gravity, together with ballistic emplacement and vortex produced by the atmosphere-ejecta curtain interaction, were essential to the (inner) layered ejecta structure formation. We hypothesize that the thinner outer layered ejecta structures were formed by various combinations of shockwave-induced liquefaction of water-rich near-surface sediments, ballistic emplacement of ejecta-entraining water, and strong winds (expanding vapor, vortex, base surge) related to the impact. The contribution of each proposed layered ejecta structure formation mechanism should have been variable depending on the condition of the impact.

Citation: Komatsu, G., G. G. Ori, S. Di Lorenzo, A. P. Rossi, and G. Neukum (2007), Combinations of processes responsible for Martian impact crater ''layered ejecta structures'' emplacement, *J. Geophys. Res.*, *112*, E06005, doi:10.1029/2006JE002787.

1. Introduction

[2] Impact craters on Mars often exhibit features that are not observed on the essentially volatile-free, airless lunar surface. The most unusual is the ejecta blanket morphology [*McCauley*, 1973; *Head and Roth*, 1976; *Strom et al.*, 1992]. Martian ejecta blankets are often characterized by a terminal low ridge (rampart), a plateau (pancake), or radial grooves. This type of ejecta morphology, collectively called ''layered ejecta structures (LESs)'' [*Barlow et al.*, 2000], is generally attributed to various ejecta emplacement processes due to the involvement of volatiles (commonly considered to be water) derived from the subsurface [e.g., *Carr et al.*, 1977; *Gault and Greeley*, 1978; *Greeley et al.*, 1980; *Ivanov and Pogoretsky*, 1996; *Barnouin-Jha et al.*, 2005] or of atmosphere [e.g., *Schultz and Gault*, 1979; *Schultz*, 1992; *Barnouin-Jha and Schultz*, 1996; *Barnouin-Jha*, 1998] or a combination of both processes [*Barlow*, 2005]. Assuming that the LES formation is linked with volatiles in the Martian crust, researchers have extensively studied the geographic dependency of LESs to estimate the distribution of the volatiles [e.g., *Kuzmin et al.*, 1988; *Costard*, 1989; *Cave*, 1993; *Costard and Kargel*, 1995; *Demura and Kurita*, 1998; *Barlow et al.*, 2001; *Reiss et al.*, 2005].

[3] In order to understand the formation mechanisms of LESs, attempts have been made to quantify various geomorphic parameters of Martian impact craters using the Mars Orbiter Laser Altimeter (MOLA) data set [e.g., *Garvin et al.*, 2000; *Mouginis-Mark et al.*, 2004]. The newly available High Resolution Stereo Camera (HRSC) data set allows high-resolution topographic analysis as well as detailed geomorphologic assessment of LESs. In this paper, we present results of our analysis of LESs utilizing the HRSC and also other data sets from previous missions. On the basis of the results, we propose our hypotheses regarding the origins of LESs.

2. Methods

[4] Our study made use of the high-resolution stereo capacity of the HRSC onboard Mars Express [*Hauber and Neukum*, 2004]. This camera enables construction of high-resolution Digital Terrain Models (DTMs) [e.g., *Oberst et al.*, 2004; *Albertz et al.*, 2005]. The derived stereo models agree

[1] International Research School of Planetary Sciences, Università "G. d'Annunzio", Pescara, Italy.
[2] ESA Research and Scientific Support Department, Noordwijk, The Netherlands.
[3] Institut fuer Geologische Wissenschaften, Freie Universitaet Berlin, Berlin, Germany.

0148-0227/07/2006JE002787$09.00

Table 1. List of Martian Impact Craters Studied Using the HRSC Data Set and Their Morphometric Characteristics[a]

Impact Crater	Coordinates	Plane of Reference With Respect to the Martian Datum, m	Crater Rim Radius, km	(Inner) LES Radius, km	Crater Cavity Volume, km^3	Maximum Depth of Crater Cavity, m	Crater Rim Height, m	(Inner) LES Thickness, m
1 (SLE)	20.5°S, 306.4°E	1100	15.8 ± 0.1	35.7 ± 0.1	680 ± 5	1050 ± 50	550 ± 10	75 ± 10
2 (SLE)	19.1°S, 306.4°E	1250	5.7 ± 0.1	10.8 ± 0.1	50 ± 5	650 ± 50	350 ± 10	110 ± 10
3 (MLE)	17.3°S, 306.5°E	1800	6.0 ± 0.1	12.5 ± 0.1	70 ± 10	900 ± 50	320 ± 10	75 ± 10
4 (SLE)	10.8°N, 323.3°E	−4700	4.6 ± 0.1	10.3 ± 0.1	39 ± 5	840 ± 50	380 ± 10	130 ± 10
5 (SLE)	5.0°N, 323.6°E	−5000	4.6 ± 0.1	9.5 ± 0.1	60 ± 10	1150 ± 50	250 ± 10	30 ± 10
6 (DLE-MLE)	6.9°N, 323.7°E	−4800	13.6 ± 0.1	27.0 ± 0.1	[b]	[b]	650 ± 10	200 ± 10
7 (SLE)	10.4°S, 306.1°E	2210	3.5 ± 0.1	7.5 ± 0.1	23 ± 5	630 ± 50	210 ± 10	80 ± 10
8 (SLE)	11.8°S, 302°E	2200	4.1 ± 0.1	8.8 ± 0.1	27 ± 5	853 ± 50	340 ± 10	129 ± 10
9 (SLE)	11.4°S, 302.6°E	2200	7.2 ± 0.1	18.0 ± 0.1	116 ± 10	1111 ± 50	350 ± 10	50 ± 10
10 (DLE)	10.2°S, 301°E	2300	3.0 ± 0.1	10.2 ± 0.1	13 ± 5	782 ± 50	220 ± 10	110 ± 10
11 (SLE)	10.5°S, 301.5°E	2300	5.6 ± 0.1	12.7 ± 0.1	52 ± 5	788 ± 50	300 ± 10	100 ± 10
12 (SLE)	10.1°S, 303.3°E	2030	5.7 ± 0.1	13.1 ± 0.1	44 ± 10	840 ± 50	170 ± 10	40 ± 10
13 (MLE)	28.3°S, 157.2°E	900	2.5 ± 0.1	8.3 ± 0.1	10 ± 5	530 ± 50	300 ± 10	82 ± 10
14 (SLE)	4.0°S, 297.1°E	1940	4.0 ± 0.1	12.6 ± 0.1	36 ± 10	890 ± 50	350 ± 10	49 ± 10
15 (SLE)	2.8°S, 297.2°E	1660	2.9 ± 0.1	6.1 ± 0.1	13 ± 5	889 ± 50	240 ± 10	73 ± 10

HRSC numbers used for the measurements (1: h0100_0000; 2: h0100_0000; 3: h0100_0000; 4: h0018_0000; 5: h0018_0000; 6: h0018_0000; 7: h0100_0000; 8: h0438_0000; 9: h0438_0000; 10: h0438_0000; 11: h0438_0000; 12: h0438_0000; 13: h0228_0000; 14: h0243_0000; 15: h0243_0000).

[a]Layered ejecta structure (LES) type classification: SLE, single-layer ejecta; MLE, multiple-layer ejecta; DLE-MLE, double-layer ejecta-multiple-layer ejecta.

[b]The HRSC image does not cover the entire crater.

with topographic data obtained earlier by the MOLA, and the HRSC effectively fills the gaps left between the MOLA shots and tracks [*Oberst et al.*, 2004]. The HRSC DTMs are calibrated using a 5-km cell size MOLA DTM during stereogrammetric processing. We investigated relatively pristine impact craters chosen from the early HRSC acquisition in order to minimize the bias caused by degradational and depositional processes (Table 1). These impact craters are distributed in eastern Tharsis, but one example from Cimmeria Terra is also included (Figure 1). The geomorphologic classifications and morphometric parameters of the studied impact craters and their associated LESs are summarized in Table 1.

[5] The measurements of various morphometric parameters of the impact craters and the LESs were conducted as follows. When both inner and outer LESs are identifiable, the much thicker inner LESs, where we have better quality of stereo-derived topographic data, were measured. The multiple-layer ejecta (MLE) type was treated as the same as the single-layer ejecta (SLE) type in our measurements. All of these measurements were performed over HRSC stereo-derived DTMs at a horizontal resolution of 100 m (oversampled to 50 m). The image processing was done with the Video Image Communication and Retrieval (VICAR) software package modified by the DLR (German Aerospace Center), and the images and the resulting DTMs were later imported into ESRI ArcGIS 8.3. The DTMs were transformed into the ESRI GRID format for various measurements. Altitudinal values were extracted from HRSC stereo-derived level 4 products.

[6] The plane of reference was taken as the mean of multiple measurements of surrounding plains elevation

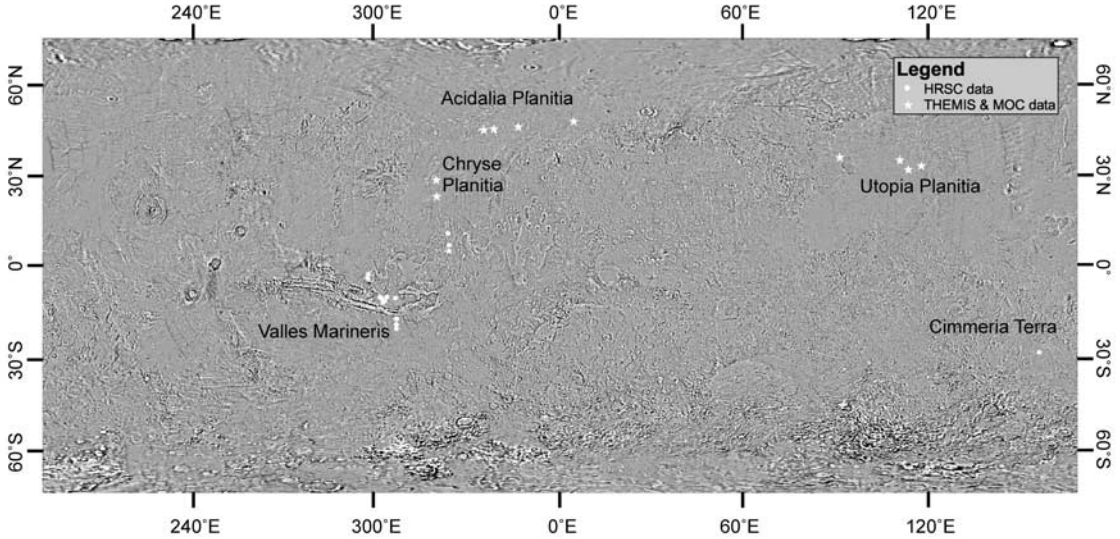

Figure 1. Locations of studied impact craters with layered ejecta structures (LESs) on Mars.

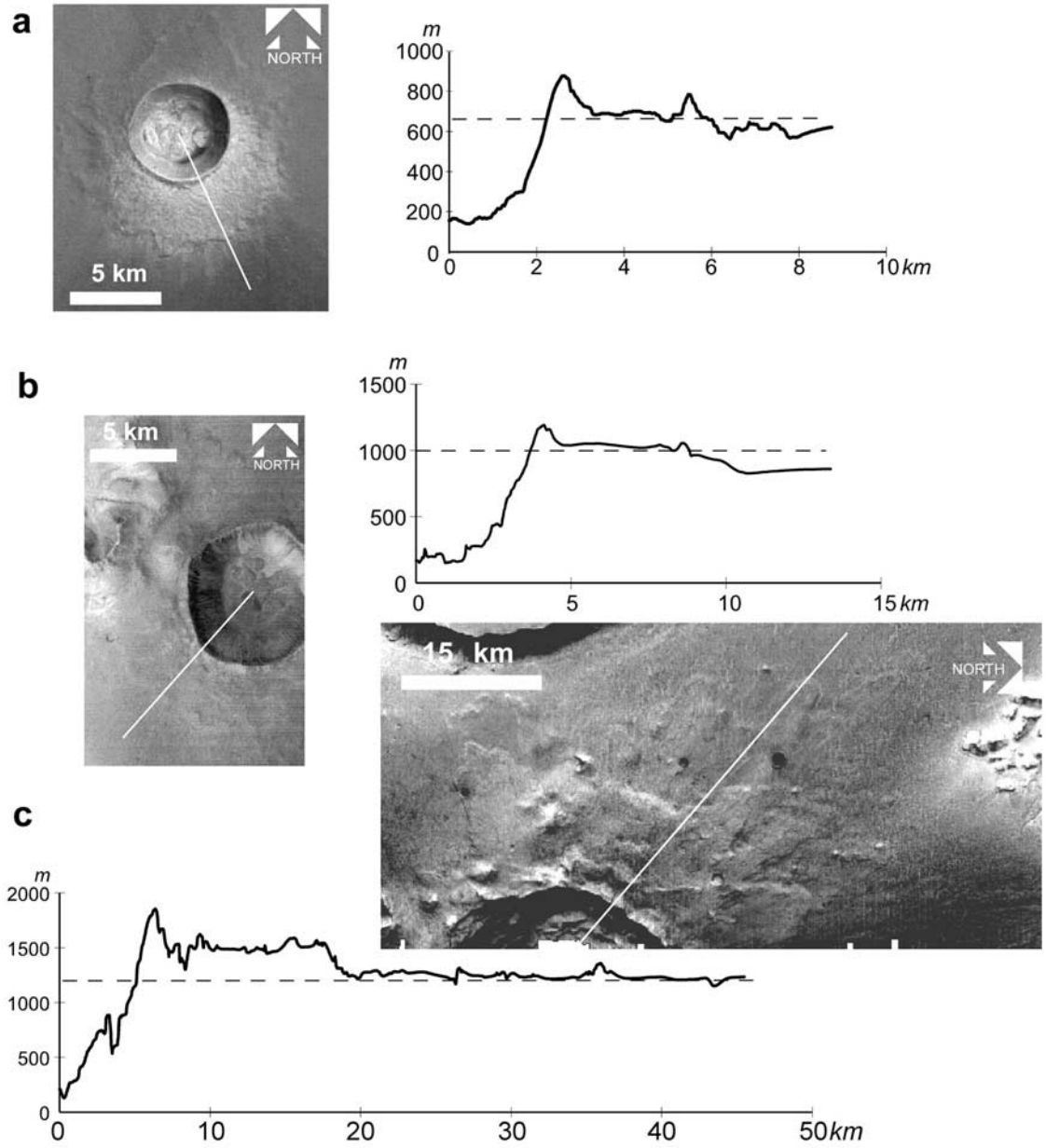

Figure 2. LES topographic profiles extracted from HRSC DTMs. Dotted lines are planes of reference. (a) A typical LES in our data set, having a plateau shape or a general trend thickening outward and a terminal rampart. Impact crater 15 in Table 1. The crater diameter is about 5.8 km. HRSC image h0243_0000. (b) A LES showing a general trend thinning outward and a rampart. Impact crater 5 in Table 1. The crater diameter is about 9.2 km. HRSC image h0018_0000. (c) An example of DLE (transition to MLE) type with petal-like lobes. Note the presence of a thicker inner LES and a thinner outer LES. Impact crater 6 in Table 1. The crater diameter is about 27.2 km. HRSC image h0018_0000.

values. The values were rounded to 10 m to discriminate spikes caused by the stereo algorithm from natural undulations in each measured point. The crater cavity and LES outline were approximated to be a circle, but when the LES margins are highly irregular, we took the average of the minimum and maximum radii. The maximum depth of the crater cavity was measured from the rim to the deepest point in the crater. The crater rim height and the (inner) LES thickness were taken as the average of multiple measurements with respect to the plane of reference. The (inner) LES thickness was measured over the continuous LESs at approximately one-half the maximum extent to avoid the influence of the rim. We note that these parameters are subject to significant errors if the chosen plane of reference does not approximate the preimpact topography of the target surface well. The crater cavity volume was measured below the rim by the ArcGIS three-dimensional analyst extension.

[7] The vertical precision of our integer stereo-derived DTMs is 1 m. The range of uncertainty (error bars) for each measurement was determined as follows: crater rim radius

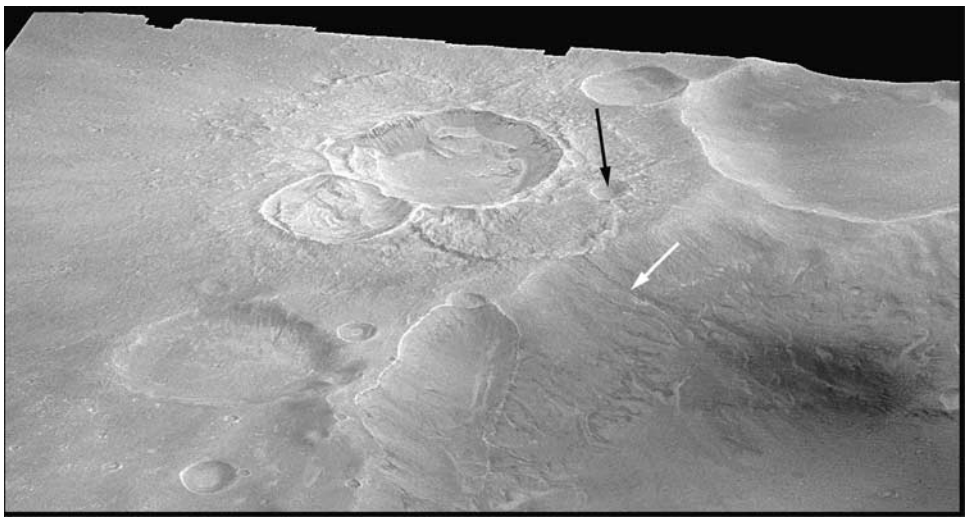

Figure 3. A double-impact crater with a LES. The LES is diverted around an old small (1.1–1.2 km in diameter) impact crater (black arrow). Channels (white arrow) emanate from the edge of the LES and end in the impact basin floor. Impact crater 7 in Table 1. The main crater diameter is about 7 km. This three-dimensional perspective view was produced by draping a HRSC image over a HRSC stereo-derived DTM. No vertical exaggeration. HRSC image h0100_0000.

and (inner) LES radius (100 m that is the nominal spatial accuracy of the stereo-derived DTMs); crater rim height and (inner) LES thickness (10 m is an accuracy to account for the minimum interval of confidence to discriminate spikes caused by the stereo algorithm from natural undulations of rim surfaces and of LES). In the case of the maximum depth of crater cavity, we used 50 m because of the larger uncertainty in distinguishing spikes and undulations on the crater floor. The estimated range of error in determining the crater cavity volume is 5 or 10 km^3 to account for the rim height variation in the DTMs.

[8] In addition to the HRSC data analysis, we utilized Thermal Emission Imaging System (THEMIS) and Mars Orbiter Camera (MOC) Narrow Angle images, and also the MOLA profile data set to study additional impact craters with LESs in Utopia, Chryse, and Acidalia planitiae (Figure 1) in order to deepen our understanding of the LES emplacement processes.

3. Geomorphological Analysis

[9] The LESs on Mars have been classified into different types including single-layer ejecta (SLE), multiple-layer ejecta (MLE), and double-layer ejecta (DLE) [e.g., *Barlow et al.*, 2000], but intermediate types exist between these classification groups (for example, impact crater 6 in Table 1). Representative topographic profiles from our HRSC study clearly show a wide range of morphology (Figures 2a–2c). Minor undulations (some of which could be artifacts) are commonly observed in the profiles. Figure 2a shows one example of typical LESs observed in our data set, which have a plateau shape or a thickening outward trend and a terminal rampart. Some LES impact craters have ejecta profiles thinning outward as shown in the example of Figure 2b, and a rampart is also observable. The thinning outward trend is what is expected for ballistic ejecta. However, the specific example in Figure 2b does not exactly match the −3 exponential decay derived for lunar craters [e.g., *McGetchin et al.*, 1973], which is presumed to represent ballistic emplacement. We also note that the actual preimpact target surface of the example in Figure 2b may have been more than 100 m below the plane of reference. The DLE type is characterized by a thicker inner LES and a much thinner outer LES (Figure 2c). Both the inner and outer LESs of DLE-type impact craters could have a terminal rampart.

[10] A double-impact crater at 10.4°S, 306.1°E shows its LES emplacement in a peculiar situation (Figure 3). This double-impact crater is located on the plateau near the edge of a degraded 40-km-diameter impact basin. The LES deposit of this crater surrounds a small impact crater (1.1–1.2 km in diameter) rather than overriding it (Figure 3). This suggests that at least part of the ejecta emplacement was ground-hugging and not simply falling from an ejecta curtain. Our HRSC image observation about the ground-hugging nature of LESs is consistent with a number of previous studies [e.g., *Carr et al.*, 1977; *Mouginis-Mark*, 1979; *Mouginis-Mark*, 1981; *Baloga et al.*, 2005]. Possible evidence for the involvement of volatiles is also found with the LES of this crater (Figure 3). Channels, probably liquid water-carved, emanate from the edge of the LES and flow into the impact basin forming a dark fan-shaped deposit.

[11] The object that formed the impact crater at 28.3°S, 157.2°E appears to have hit at the edge of 400- to 500-m-high walls of an impact basin. This crater exhibits a rather unique situation in terms of LES morphology (Figure 4). The flow-like features originating from the crater and emplaced in the basin are characterized by 50- to >100-m-thick multiple lobes with longitudinal grooves visible on their upper surfaces. This type of groove is also observed with large landslide debris aprons commonly emplaced on the floors of Valles Marineris canyons [*Lucchitta*, 1987], and they are often interpreted to have formed moist or wet [e.g., *Lucchitta*, 1987]. These lobes may have formed as wall-derived landslides triggered by the impact event, but

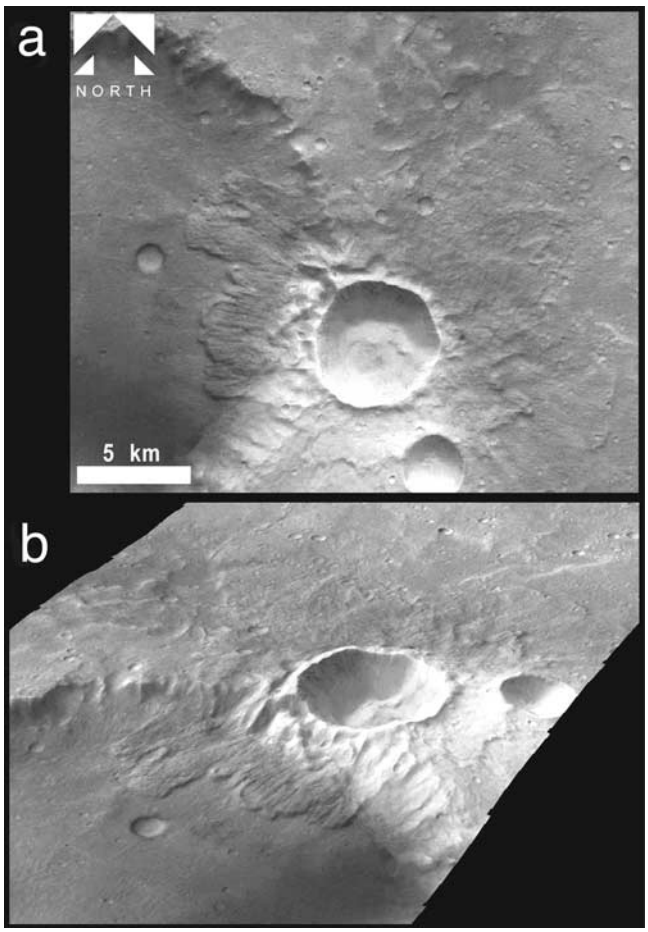

Figure 4. This impact crater with a LES is positioned on the edge of 400- to 500-m-high walls of an impact basin. Note that the LES lobes emplaced on the basin floor are longitudinally grooved. Impact crater 13 in Table 1. The crater diameter is about 5 km. (a) Plan view. (b) This three-dimensional perspective view was produced by draping a HRSC image over a HRSC stereo-derived DTM. Vertical exaggeration 2. HRSC image h0228_0000.

they are considered to be parts of the LES on the basis of their continuation to the rest of the LES. In any case, this example again indicates that the LES emplacement was ground-hugging, and it is possible that volatiles were involved.

[12] Some LESs have asymmetrical patterns (Figure 5). Their patterns are not always bilaterally symmetric as expected from very oblique impacts. This implies that beside the angle of impact, there are other factors affecting the ejecta distribution.

[13] Observations of relatively pristine LESs (both SLE and DLE types) by THEMIS visible (VIS) data provided insights on the formation of radial or near-radial striations [e.g., *Mouginis-Mark*, 1981; *Boyce and Mouginis-Mark*, 2006] frequently visible on the surfaces of LESs (on both inner and outer LESs in the case of the DLE type). The presence of the striations passing across thicker inner and thinner outer LES surfaces has been used as an indication of prior formation of the inner layer, subsequent sweeping by the outer layer across the inner layer, producing the striations on the inner layer, and formation of the outer layer LESs [e.g., *Mouginis-Mark*, 1981; *Boyce and Mouginis-Mark*, 2006]. Some well-preserved radial striations are visible in one example of LES impact craters (Figure 6a). These striations are straight over the LES surface, and the edge of the LES appears to be modified. Individual striations (either grooves or ridges) are occasionally traceable from the LES surface to its outside. Extensions of the striations are observed as discontinuous ridges outside the LES edge, implying that whatever the processes formed the striations modified the LES surface and deposited some materials outside the LES. A possibility that the striation-producing processes have carried materials derived from the excavated cavity also exists. Such extensions of striations coalesce to form more continuous materials (Figure 6b) or sinuous lobes in some instances (Figure 6c). These examples indicate that the striation-producing processes transported significant amounts of materials and deposited outside of the original LESs. However, it is also possible that the striation-producing

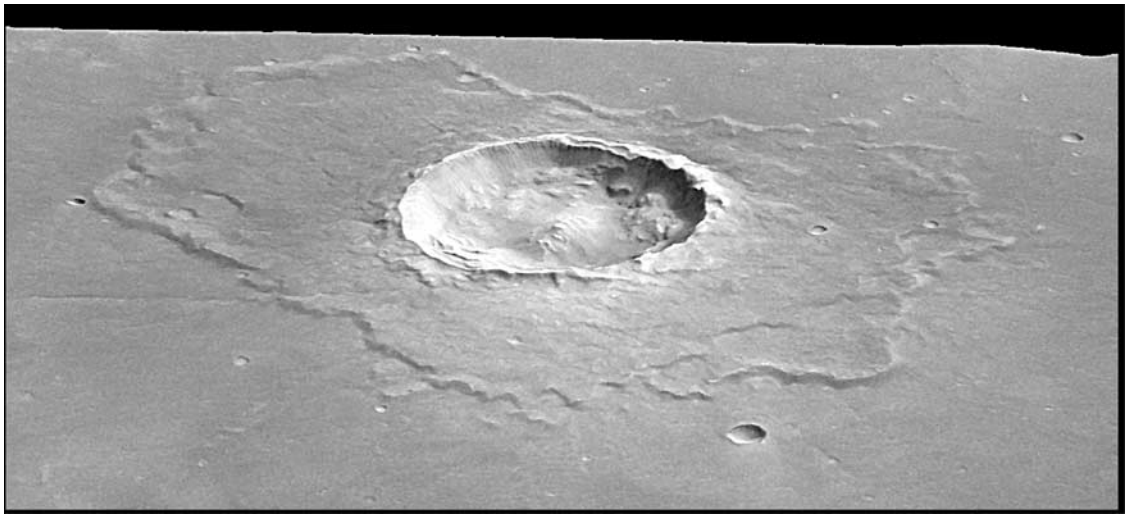

Figure 5. An impact crater with an asymmetrical LES. Impact crater 9 in Table 1. The crater diameter is about 14.4 km. This three-dimensional perspective view was produced by draping a HRSC image over a HRSC stereo-derived DTM. Vertical exaggeration 1.5. HRSC image h0438_0000.

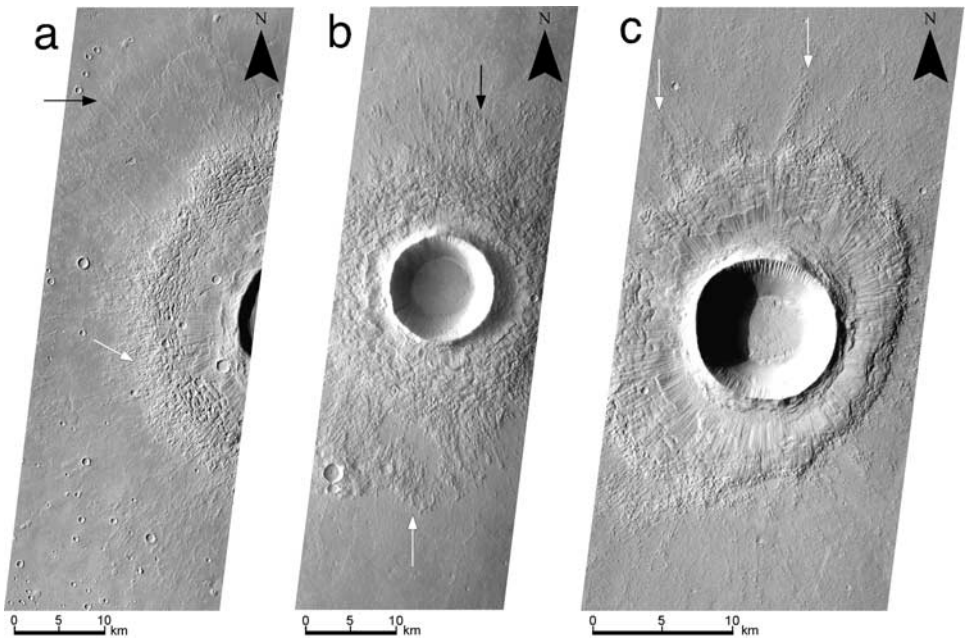

Figure 6. Various striation morphology observed at impact craters with LESs (a) Striations are straight over the LES of this impact crater (35.8°N, 91.8°E in Utopia Planitia), and they extend out of the LES (white arrow). The edge of the LES seems to be modified by the striation-forming processes. The transported materials are deposited away from the LES (black arrow). The crater diameter is about 12 km. THEMIS VIS image V12117002. (b) This impact crater (34.9°N, 111.6°E in Utopia Planitia) has striations. It seems that abundant materials were transported by the striation-producing processes and deposited near the LES (black arrow). Some materials may have accumulated at some distances from the main LES (white arrow). The crater diameter is about 11.5 km. THEMIS VIS image V14138009. (c) This impact crater (31.8°N, 114.3°E in Utopia Planitia) has striations. It seems that materials transported by striation-producing processes and deposited as sinuous lobes (white arrows). The crater diameter is about 10 km. THEMIS VIS image V12840007.

processes modified the continuous materials and sinuous lobes, which were formed earlier in the impact cratering.

[14] A DLE-type impact crater called Bacolor in Figure 7a was studied in detail by *Mouginis-Mark* [1981], *Boyce and Mouginis-Mark* [2005], *Mouginis-Mark and Boyce* [2005] and *Boyce and Mouginis-Mark* [2006]. It has an asymmetric outer LES; continuous from the inner LES without a clearly defined edge of the inner LES in the northeast direction (Figure 7b), discontinuous (with clearly defined terminal ramparts) to the north/northwest direction (Figure 7c), and continuous but with a clearly defined edge of the inner LES in the south/southeast direction (Figures 7d and 7e). The striations on the inner LES are radial with respect to the crater center and straight, but the striations observed on the outer LES (Figures 7b–7e) are more sinuous or channel-like as observed by Boyce and Mouginis-Mark and Mouginis-Mark and Boyce. The striations observed on the outer LES in the northwest direction of the crater incise into the terminal ramparts, and materials are deposited outside of the terminal ramparts (Figure 7c). Some striations, particularly in the south direction, are clearly traceable from the edges of inner LES lobes to the surfaces of outer LES lobes (Figure 7d). The edges of the inner LES lobes are rather sharp here, but partial collapsing of the edges appears to have formed extended lobes. The striations (sinuous grooves or ridges) either fill or cut preexisting impact craters on the outer LES lobes in the south/southeast direction (Figures 7d and 7e). We also note that thin flow-like features characterized by fine ridges are superposed on the outer LES lobes and also visible outside of them (Figure 7e).

[15] The partial collapsing and ground-hugging nature of inner LES emplacement are observed also in other examples (e.g., Figure 8a). In the case of at least one DLE-type impact crater (Figure 8b), its inner LES is observed to clearly override the outer LES, and striations seem to be continuous from the inner to the outer LES surfaces, implying formation of the striations later than both the outer and the inner LESs.

[16] In summary, our observations confirm the previous works about the detailed morphology of the striations. And some fractions of outer LESs seem to be composed of materials transported by the processes that formed the striations. However, the order of formation among the thicker inner LESs, the thinner outer LESs, and the striations is not clearly established for the majority of cases in our observations. We think that the stratigraphic relationship between the inner and outer LESs may not be uniquely determined for the majority of cases without investigating across their boundaries by methods such as radar, seismic survey, and trenching. Striations could have formed after the emplacement not only of the inner LESs but also of the outer LESs, leaving a possibility that these outer LESs formed before the inner LESs at least in some cases. We also note that the outer LESs exhibit a wide range of morphology, strongly implying more than one mode of formation.

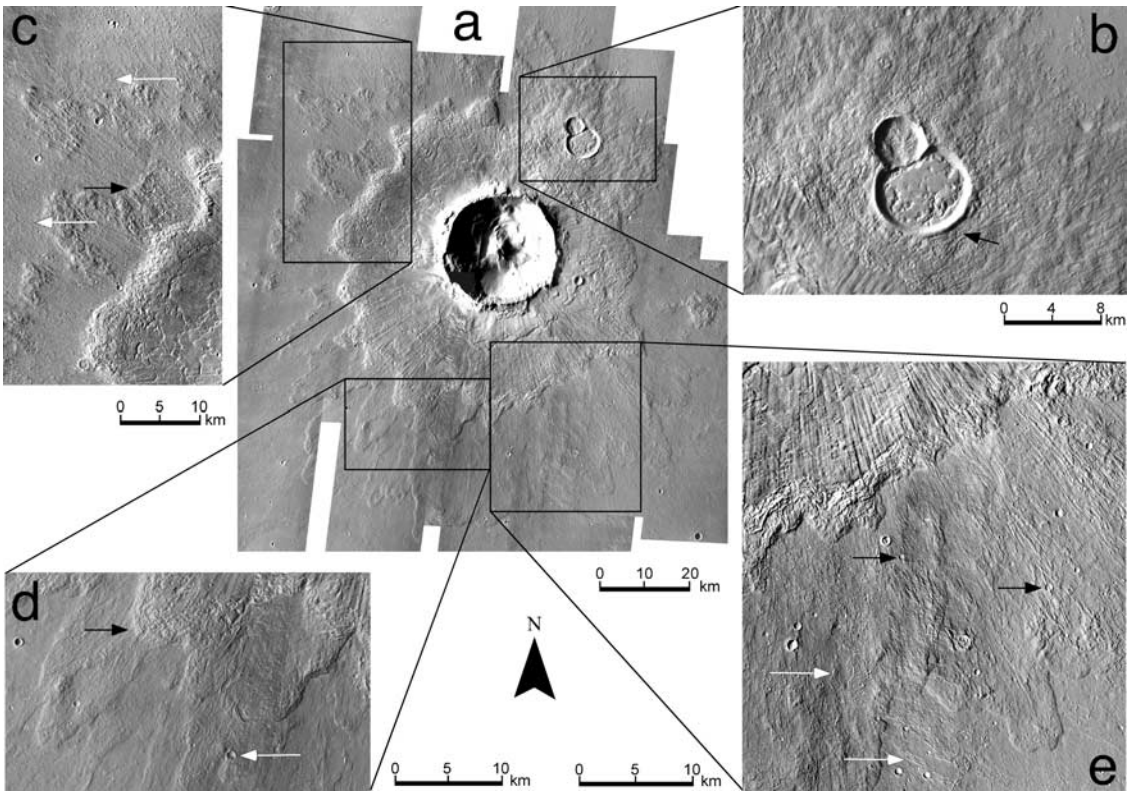

Figure 7. (a) The Bacolor impact crater (33°N, 118.6°E in Utopia Planitia) is characterized by an asymmetric outer LES and striations. The striations are in general straight on the inner LES but sinuous or channel-like on the outer LES. (b) The outer LES in the northeast direction is continuous from the inner LES. Striations on the inner LES are straight, but the ones on the outer LES are more sinuous, diverting around a preexisting double-impact crater (black arrow). (c) The outer LES in the north/northwest direction is discontinuous from the inner LES and is characterized by clearly defined terminal ramparts that are cut by the striations (e.g., black arrow). Some materials are deposited outside of the terminal ramparts (white arrows). (d) The outer LES in the south direction is characterized by the lobe morphology. Some striations are traceable from the edges of the inner LES lobes to the surfaces of the outer LES lobes (black arrow). The materials related to the striation formation appeared to have entered one preexisting impact crater and flowed out (white arrow). (e) The outer LES in the southeast direction is characterized by the lobe morphology. Striations (sinuous grooves or ridges) either fill or cut preexisting impact craters (black arrows). Thin flow-like features characterized by fine ridges are superposed on the outer LES lobes and also visible outside of them (white arrows). The crater diameter is about 24 km. THEMIS VIS mosaic images V11854007, V17682033, V10319007, V12428008, V11829005, V17657026, V13364007, V13052008, V13988002, V12453007, V13676010, V09670012, V13077006, V10294008, V05114012, V17058008, V12765007, V12141005, V13963010, V05451015, and V14300012.

[17] DLE-type impact craters at mid latitudes, particularly in Acidalia Planitia, are often characterized by outer LESs with undulating surfaces and associated by mounds of various sizes within the areas of the outer LESs or in their vicinity (e.g., Figure 9a). The undulating surfaces may be a result of secondary modifications such as periglacial processes. However, it is also possible that they originated in impact cratering. At least in one case, the edge of the outer LES exhibits flow-like lobes or appears to transition to coalescced mounds (Figure 9a), implying a continuum of processes that were responsible for the formation of the outer LES and the mounds. Faint radial striations are observed on both the inner and the outer LESs, but whether they are continuous over both the LESs is not clear. In another example, a smooth light-toned material appears to have emanated from a DLE-type impact crater and ponded in low-lying areas (Figure 9b). "Pancake" features that are quasi-circular relatively flat and made of material with its albedo higher than the surroundings [*Farrand et al.*, 2005] appear to fill depressions near the crater (Figure 9b). In order to elucidate on the process of formation of such outer LESs in Acidalia Planitia, detailed observations of the DLE type were made (Figures 10, 11, and 12) using THEMIS, MOC, and MOLA profile data. The two impact craters we investigated in detail are located in two separated areas within mottled plains of Acidalia Planitia (Figure 1). Many DLE-type impact craters occur in close vicinity of the studied craters.

[18] A DLE-type impact crater (47.5°N, 4.8°E) (Figure 10a) has an inner LES with a radius of about 25 km and an outer LES with a radius of about 40 km (both were measured from the crater's center point). The surface of the outer LES is

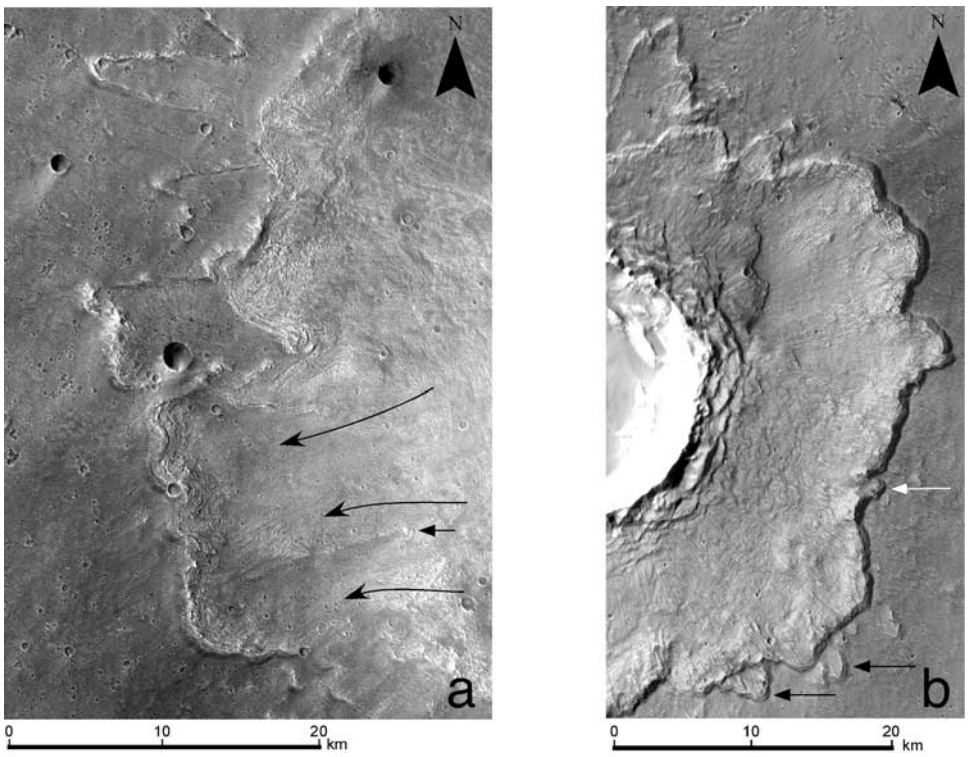

Figure 8. (a) Partial collapsing of the edge of the inner LES (long arrows) is observed with this impact crater (23°N, 319.7°E in Chryse Planitia). The resulting flow was ground-hugging as indicated by flow lines diverting around a small topographic obstacle (short arrow). The crater diameter is about 20 km. THEMIS VIS mosaic images V10287007 and V17650023. (b) The inner LES of this impact crater (28.4°N, 319.5°E in Chryse Planitia) appears to override outer LES lobes (black arrows). Striations are continuous from the surfaces of the inner to the outer LES, implying a later formation of the striations. A small collapsing feature of the inner LES edge is observed (white arrow). The crater diameter is about 17.5 km. THEMIS VIS mosaic images V12446004 and V10599013.

undulated. A MOC image reveals that radial striations are observed on the inner LES, but they are not clearly visible on the outer LES (Figure 10b). Surfaces of both the inner and outer LESs are partially characterized by small pits of tens of meters across, which appear to be ice sublimation features. Both the inner and the outer LESs have well-defined lobes at their toes. The inner LES also has a broad low terminal rampart as shown in the MOLA profile (Figure 10c), resulting in a moat between the crater's rim crest and the rampart. Thermal properties of LESs could offer information regarding the state of LES surface conditions [*Betts and Murray*, 1993; *Baratoux et al.*, 2005]. The THEMIS nighttime infrared (IR) image of the same impact crater shows that the inner LES has a brighter surface compared with the surface of the outer LES (Figure 11). This means that the inner LES surface is characterized by higher thermal inertia values in comparison to the outer LES surface. It is the trend observed also for some DLE impact craters in Syrtis Major [*Baratoux et al.*, 2005]. This observation can be interpreted that the inner LES surface is made of coarser-grained materials than the outer LES surface.

[19] Small impact craters (up to several kilometers in diameter) with well-defined ejecta blankets are observed near the crater (Figure 10a). Their rim and ejecta surfaces are bright in the THEMIS nighttime image (Figure 11), which is consistent with the expected presence of relatively coarse ejecta materials on their surfaces. Mounds of about a few hundred meters to a few kilometers in diameter occur widely in the vicinity of the crater (Figure 10a). We note that the resolutions of the images prohibit us from identifying mounds smaller than a few hundred meters across. In contrast to their surroundings and the small impact craters in the area, these mounds are very dark in the THEMIS nighttime image (Figure 11). This probably indicates that their surfaces are made of relatively fine-grained materials, which is consistent with the estimated grain sizes (basaltic fine to coarse sands) of similar mounds in Acidalia Planitia [*Farrand et al.*, 2005]. Similar mounds are widespread also in other parts of Acidalia Planitia, and their abundant presence contributes to the mottled-appearing surfaces.

[20] Another DLE-type impact crater (44.5°N, 335.3°E) is also insightful in understanding the processes related to the outer LES formation (Figure 12). This crater is one of many DLE-type impact craters occurring in mottled and polygonally fractured plains south of Acidalia Mensa. The outer LES in the northern side of the crater exhibits a fragmented appearance (Figure 12a) as the fragmented pieces of the LES are clearly separated from the main continuous LES. They have well-defined margins rather than gradational margins that are expected from erosional processes. Although we cannot rule out the possibility that they are erosional remnants of an originally continuous ejecta deposit, it seems that these pieces of the LES were emplaced separately from the main continuous LES, and post-impact erosion was not the main cause for this frag-

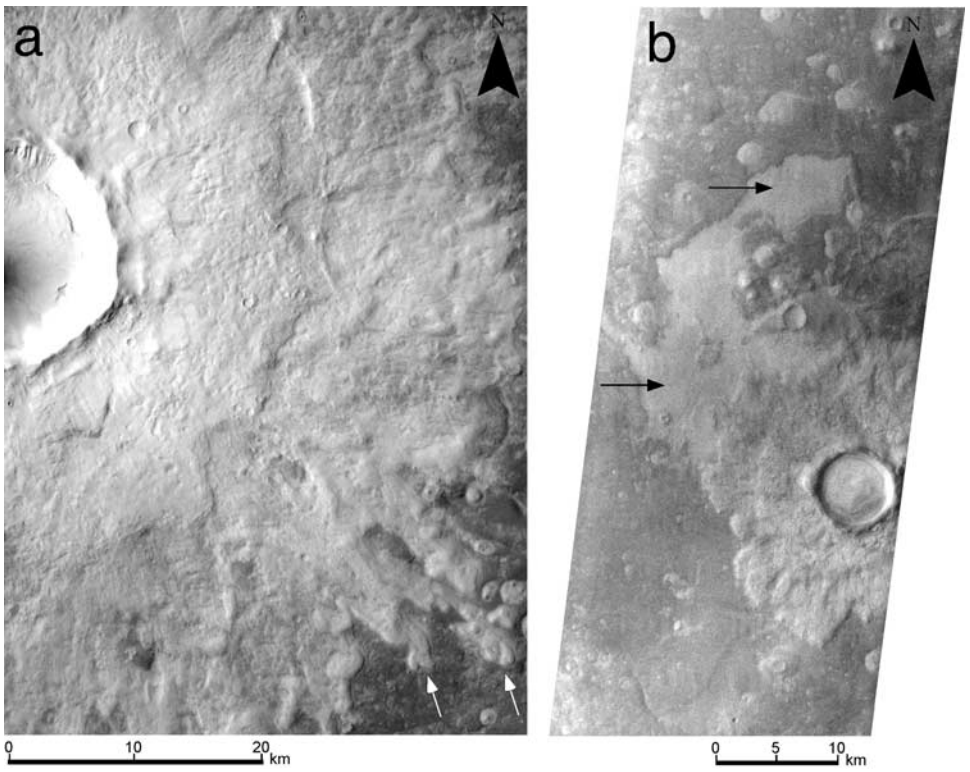

Figure 9. Impact craters in Acidalia Planitia often exhibit outer LESs with undulating surfaces, and mounds are observed in their vicinity. (a) This DLE-type impact crater (45.8°N, 346.4°E in Acidalia Planitia) has an outer LES with an undulating surface. Mounds are distributed near the outer LES. The edge of the outer LES exhibits flow-like lobes or appears to transition to coalesced mounds (white arrows). The crater diameter is about 18 km. THEMIS VIS mosaic images V04457004 and V05206007. (b) This DLE-type impact crater (45.1°N, 338.4°E in Acidalia Planitia) is associated with an extensive area of smooth light-toned material (black arrows). "Pancake" features that are quasi-circular, relatively flat and made of material with its albedo higher than the surroundings appear to fill depressions near the crater. The crater diameter is about 6 km. THEMIS VIS image V14255010.

mented appearance. This impact crater is surrounded by mounds of about a few hundred meters to a few kilometers in diameter (Figure 12a). The mounds appear to be dome- or cone-shaped, and some of them have a summit crater as identified in a high-resolution MOC image (Figure 12b). Mounds of a small size range (a few hundred meters) are observed also inside the zone of the outer LES (Figure 12a). Our examination of a THEMIS nighttime infrared (IR) image (I05350014) revealed that the mounds' surfaces are characterized by a lower thermal inertia range compared to their surroundings, which is consistent with what we found in the other area (Figure 11).

4. Morphometric Analysis

[21] The number of impact craters examined in our morphometric analysis is 15. The examined properties of these morphologically pristine-appearing impact craters are derived from HRSC high-resolution three-dimensional topographic data. The nature of this data set allows us a precise quantitative analysis. However, we caution that any morphometric analysis of impact craters on Mars could be affected by degradation since virtually no Martian impact crater is totally free of erosion or burial. Furthermore, many of the impact craters we sampled from the early HRSC acquisition occur on nonhorizontal terrains or are affected by local topography (massifs, cliffs, etc.). Some are double crates or have highly irregular LESs. All these conditions may have led to inaccurate measurements. Incomplete HRSC spatial coverage of some impact craters and their LESs was also a problem. Future works should examine much larger numbers of samples occurring in conditions as ideal as possible.

[22] Two positive correlations (crater rim radius versus crater cavity volume, crater rim radius versus LES radius) are clear (Figures 13a and 13b). The positive relationship between the crater rim radius and the crater cavity volume implies that the states of burial for these impact craters are not drastically different from each other. It is consistent with their relatively pristine (nonburied) appearances inferred from geomorphology.

[23] The positive relationship between the crater rim radius and the LES radius (thicker inner LES in the case of the DLE type) shows that the emplacement of LESs within our samples was controlled primarily by the impact energy (the larger the energy is, the farther the LES extends). The regression line for the crater rim radius (R) versus the LES radius (R_LES) plot is

$$R\_LES = 2.03R + 1.54 \quad (1)$$

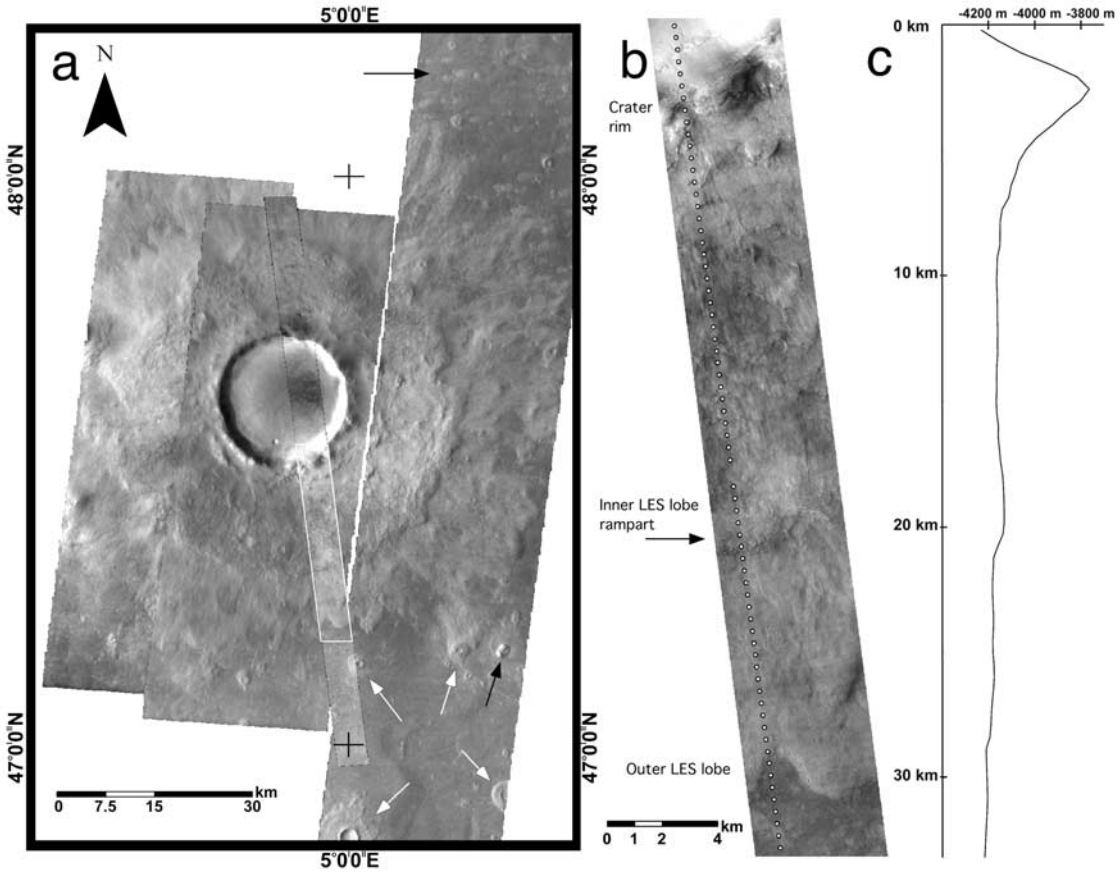

Figure 10. An example of DLE-type impact craters (47.5°N, 4.8°E in Acidalia Planitia). (a) The surface of the outer LES is undulated. Small impact craters (up to several kilometers in diameter) with well-defined ejecta are observed near the crater (white arrows). In the vicinity of the crater, there are many small mounds (a few hundred meters to a few kilometers in diameter) occurring outside the outer LES (one field of such mounds is indicated by a black arrow to the northeast). The largest mound in the area and its associated flow-like materials are indicated by a black arrow to the southeast. The crater diameter is about 20 km. The position of the MOC image (Figure 10b) is shown (white frame). THEMIS VIS mosaic images V13992003, V10011002, and V10635009. (b) An arrow indicates the terminal rampart of the inner LES, which approximately coincides with the boundary between the inner LES and the outer LES. Both the inner and outer LESs are characterized by lobes at their toes. Faint radial striations are visible on the inner LES but not clearly visible on the outer LES. The dotted line indicates the position of the MOLA track shown in Figure 10c. MOC Narrow Angle image E0401261. (c) The MOLA profile crossing over the area of Figure 10b (dotted line) shows that the inner LES thickens outward, forming a low rampart. The thinner outer LES is also identifiable in the profile. MOLA raw profile on the PEDR file AP19789l.b.

which is close to

$$R\_\text{ejecta} = (2.3 \pm 0.5)R^{1.006} \tag{2}$$

obtained by *Moore et al.* [1974] for lunar craters (R_ejecta is radius of the ejecta blanket). This indicates that the ratio of the ejecta range to the rim radius for the (inner) LESs in our studied samples are approximately the same as in the case of the ratio of the observed ballistic ejecta range to the rim radius on the Moon.

[24] The LES (inner LES in the case of the DLE type) thickness measurement at one-half the extent of ejecta shows an interesting result (Figure 13c). The LESs of the impact craters we examined are thicker than the ejecta thicknesses derived for the same size lunar craters [*McGetchin et al.*, 1973], which is expressed in the equation,

$$\delta = 0.14\,R^{0.74}(r/R)^{-3.0} \qquad \text{for } r \geq R \tag{3}$$

where r is the radial distance from the crater center and R is the crater radius (units are in m). Here this equation is presumed to represent ballistic emplacement. The large differences in LES thickness (even taking into account the fact that equation (3) was derived for lunar craters) indicate that the formation of the (inner) LESs was not simple ballistic emplacement. Such difference may be caused by the emplacement of ejecta materials preferentially away from the crater rim in comparison to the simple ballistic emplacement. Differences in thickness between Martian

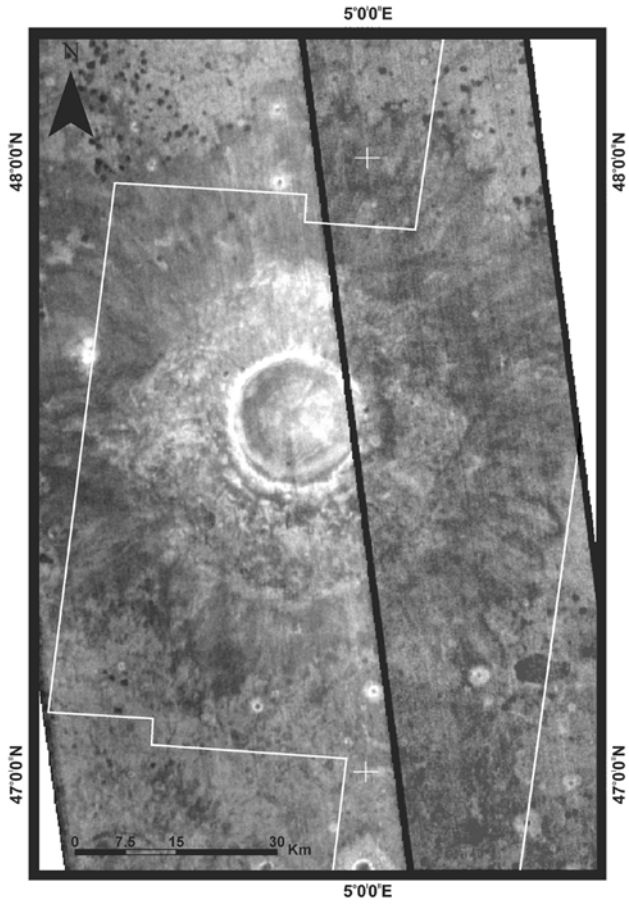

Figure 11. This THEMIS nighttime IR image of the impact crater in Figure 10 shows that the inner LES is brighter than the outer LES, indicating that the inner LES surface is characterized by higher thermal inertia than the outer LES surface. It is likely that the surface of the inner LES is composed of coarser-grained materials than the outer LES surface. The rim and the well-defined ejecta of small impact craters are bright in the image, which is consistent with the expected high thermal inertia (relatively coarse-grained) materials on their surfaces. Mounds existing outside the outer LES are much darker than the surroundings and the small impact craters, implying that their surfaces are made of relatively low thermal inertia (relatively fine-grained) materials. The position of the THEMIS VIS mosaic image (Figure 10a) is shown (white frame). This black-and-white image was converted from a Red, Green, Blue (RGB) image made of bands 4, 9, and 10. THEMIS nighttime IR images I05324011 and I06048007.

impact crater ejecta and predicted ballistic ejecta have been noted also in other works [*Garvin and Frawley*, 1998; *Garvin et al.*, 2000; *Barnouin-Jha et al.*, 2005; *Stewart and Valiant*, 2006].

[25] No evident correlation between the crater rim height and the (inner) LES thickness exists in our data (Figure 13d). The rim height, which is related to the impact energy and the influence of gravity, may be important, but it is probably not exclusively determinant for the thickness distribution (and possibly the volume) of the (inner) LESs. This result could indicate that other factors such as the amount of volatiles and preimpact surface topography may have also affected the formation of the (inner) LESs.

5. Discussion

5.1. Formation Mechanisms of (Inner) Layered Ejecta Structures

[26] The LESs (inner LESs in the case of the DLE type) we studied are often characterized by ground-hugging flows (Figures 3, 4, and 8a) and the presence of unusual topographic profiles, including ones that are plateau-shaped or thickening outward (e.g., Figure 2a). They do not follow the thickness variation of simple ballistic ejecta (Figure 13c). These properties of the (inner) LESs, if they are original pristine forms, clearly indicate that the LES emplacement was not simply ballistic deposition of ejected materials.

[27] A vortex ring made of winnowed fine particles would form behind an outward-moving ejecta curtain in the atmosphere [*Schultz and Gault*, 1979; *Schultz*, 1992; *Barnouin-Jha and Schultz*, 1996; *Barnouin-Jha*, 1998]. Such atmosphere-ejecta curtain interaction process inevitably operates on Mars. And the consequent turbulent flow may have influenced the ballistic ejecta and distributed ejecta materials. The possible modes of ejecta emplacement due to the atmosphere-ejecta interaction are complex as summarized by *Schultz* [1992]. However, it is uncertain if the atmosphere-ejecta curtain interaction process (taking into consideration also the effect of vapor plume produced by the impact) alone can explain the wide range of (inner) LES morphology and the highly asymmetrical patterns of some (inner) LES emplacement. *Osinski* [2006] also notes that there is no clear evidence to date for the interaction of the atmosphere during ejecta deposition in the known terrestrial impact-cratering record.

[28] We think that significant fractions of the (inner) LES formations were due to fluidized ground-hugging movement of ballistic ejecta and of crater rim materials that were structurally uplifted (Figure 14). Debris can initiate movement outward from the raised rim, a process discussed also by other researchers [e.g., *Schultz*, 1992; *Barnouin-Jha et al.*, 2005]. The ground-hugging movement of such flows was likely facilitated by fluidization caused by the presence of volatiles (most likely water), although the process of dry granular flows may not be totally ruled out [*Barnouin-Jha et al.*, 2005]. The ballistic ejecta materials were probably emplaced before the occurrence of ground-hugging flows in this mechanism. The ballistic materials including ones projected far away from the rim area, if they were able to keep volatiles from the excavated zone [e.g., *Carr et al.*, 1977] or to incorporate volatile-rich surficial target materials by ballistic sedimentation [*Osinski*, 2006], may have produced fluidized ground-hugging flows. We consider that volatiles were available also from within the uplifted part of the rim, and this part also contributed to the ground-hugging flows. The flows originated near or at the rim may have overriden distal areas of the LESs, which could explain the observation in Figure 8b. The ratio of pure ballistic to volatile-assisted ground-hugging components increases for the impacts in volatile-poor target materials, possibly explaining more ballistic-type ejecta profiles (e.g., Figure 2b).

[29] The ground-hugging (inner) LES flows may have originated with the momentum provided by the impact

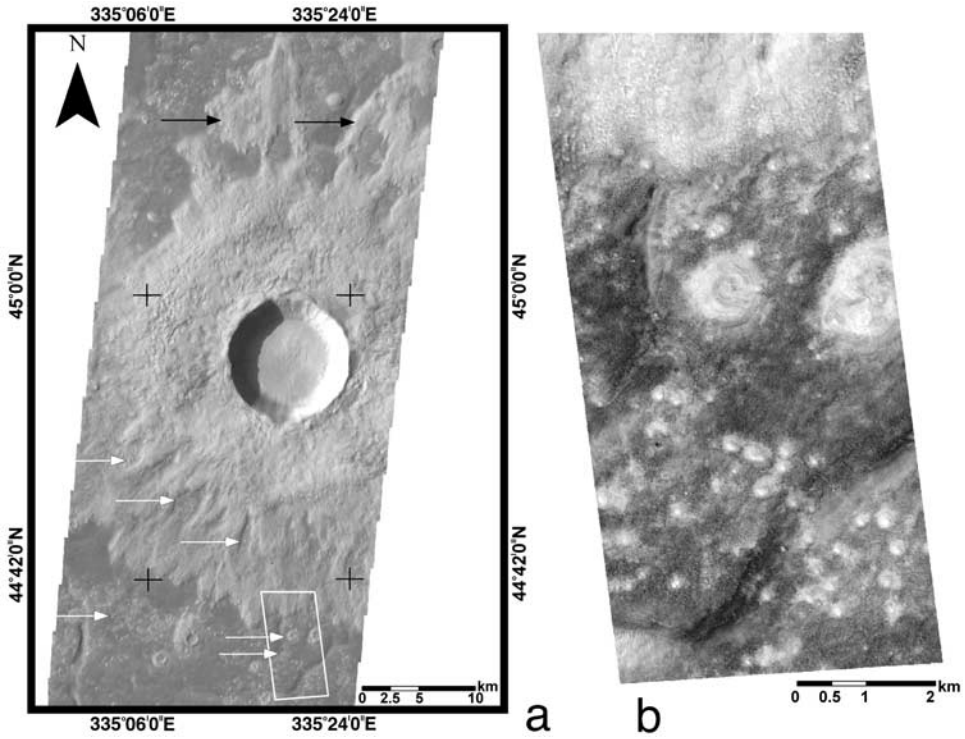

Figure 12. An example of DLE-type impact craters (44.5°N, 335.3°E in Acidalia Planitia). (a) The outer LES on the northern side of the crater has a fragmented appearance (black arrows). Their emplacement seems to have occurred separately from that of the main continuous LES component. The sinuous trenches observed around the crater are polygonal fractures commonly occurring in the region. There are many mounds widely distributed in the vicinity of the crater, and some of them occur inside the zone of the outer LES (white arrows). The crater diameter is about 10 km. The position of the MOC image (Figure 12b) is shown (white frame). THEMIS VIS image V13394006. (b) Mounds appear to be dome- or cone-shaped in general, and some have a summit crater. MOC Narrow Angle image R1901750.

explosion, and the gravity potential given by the height of rim probably assisted in their movement outward. The gravitationally driven component in the ground-hugging flows was stressed also by *Mouginis-Mark and Baloga* [2006]. We believe that additional factors may have played important roles as implied from Figure 13d. In particular, the LESs were probably fluidized by volatiles. The volatiles likely included not only vaporized water but also meltwater or preexisting liquid water. The involvement of water may be indicated by the channels emanating from the edge of the LES (Figure 3), which appear to have been formed by incision of the water escaping from the LES. Other crustal volatiles such as CO_2 and methane may also have played some roles. In addition to the excavation zone and volatile-rich surficial target materials, an important source of water may have been the uplifted part of the rim. Up to one half of the raised rim for a transient crater may be formed by structural uplift [*Melosh*, 1989, page 87], and the uplifted part of the rim could have contained liquid water that was not vaporized.

[30] Water either in ice or liquid form stored in the subsurface can be liberated because of impact excavation. Water ice can be melted owing to impact-induced shock [*Stewart and Ahrens*, 2003]. Numerical modeling by *Stewart et al.* [2004] shows that for typical impact events, in the present climate on Mars, extensive melting of groundwater ice can occur within the excavation zone, but only limited melting would occur in the rim. We think that liquid water may have been available for the LES flows also for other reasons. There are enormous uncertainties about the present crustal distribution of both water ice and liquid water [*Clifford*, 2003], let alone in the geological past. Furthermore, *Travis et al.* [2003] showed that subsurface hydrothermal convection driven by background geothermal heating might significantly thin the permafrost ice layer on Mars, bringing the liquid water close to the surface. Shallow aquifers in the crust may occur on Mars owing to the presence of potent freezing-point depressing salt components that may maintain near-surface or even surface liquid water [*Kargel and Marion*, 2004]. Dehydration of hydrous salts may also release large quantities of water [*Montgomery and Gillespie*, 2005].

[31] Water-rich sediment flows can take a variety of forms depending on the sediment concentration and grain size [e.g., *Allen*, 1997]. And liquid water in the ejecta would greatly enhance the mobility of the ejecta debris [*Melosh*, 1989; *Ivanov*, 1996; *Ivanov and Pogoretsky*, 1996]. Attempts have been made to model water-involved Martian ejecta emplacement processes [e.g., *Ivanov*, 1996; *Ivanov and Pogoretsky*, 1996]. The basal sliding model somewhat similar to our proposed emplacement mechanism was found by *Barnouin-Jha et al.* [2005] to fit well with the morphology of the near-rim region of fluidized ejecta. They also noted that the oversteepened rim due to impact into water-rich targets could have been the source of the flows. The

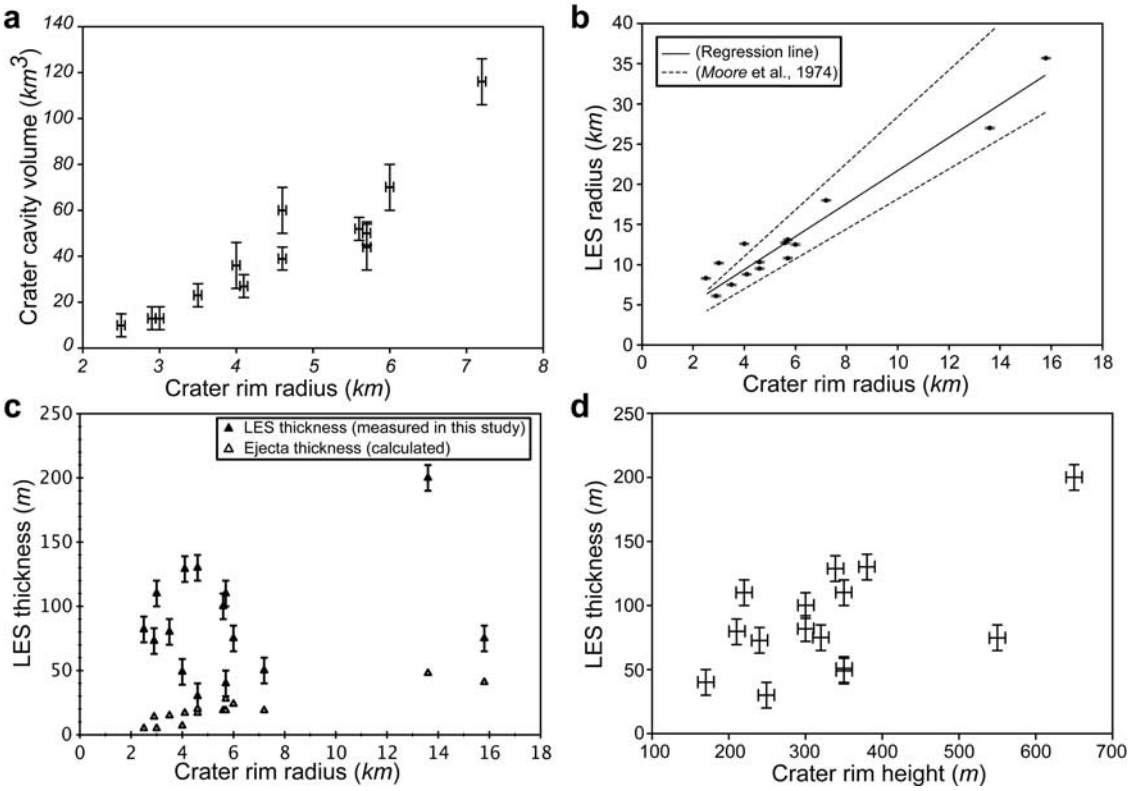

Figure 13. Plots of various morphometric parameters of the studied impact craters with LESs. (a) Crater rim radius versus crater cavity volume. The error bar associated with the crater rim radius shows the horizontal accuracy of the DTMs. The error bar for the crater cavity volume shows the range of error in the estimation of the volume. The data points for impact crater 1 and impact crater 6 in Table 1 are excluded from this plot because of the volume value too large for plotting (impact crater 1) and a lack of volume data (impact crater 6). (b) Crater rim radius versus (inner) LES radius. The error bars associated with the crater rim radius and the (inner) LES radius are the horizontal accuracy of the DTMs. However, the error bar for the crater rim radius is not plotted to make the error bar for the (inner) LES radius legible. Regression line for our data (solid line) and upper/lower bounds for lunar craters (dotted lines, from *Moore et al.* [1974]) are also shown. (c) Crater rim radius versus (inner) LES thickness. The error bar associated with the crater rim radius is the horizontal accuracy of the DTMs, but it is not shown to avoid a congested plot. The error bar associated with the LES thickness shows a vertical accuracy in the measurement. The comparative ejecta thickness values were derived on the basis of the equation given by *McGetchin et al.* [1973] at one half of the LES extent. (d) Crater rim height versus (inner) LES thickness. Both the error bars associated with the crater rim height and the LES thickness are vertical accuracies in the measurements.

plateau shape can be explained by the halting of a flow with relatively low turbulence, although postimpact erosion cannot be ruled out for the partial production of this morphology. The terminal rampart morphology probably resulted from the accumulation effect at the front of the LES as it comes to stop. *Baloga et al.* [2005] showed that frictional resistance of a continuum overland flow form ramparts naturally because of the cylindrical geometry. We add that the crustal structure with heterogeneous distributions of water reservoirs could vary widely at the time of impact, and together with preimpact surface topography and the angle of impact, this could account for the wide variation of the (inner) LES morphology (e.g., Figures 2a, 2b, and 5). This idea is consistent with previous inferences [e.g., *Kargel*, 1986; *Barlow*, 1994; *Baratoux et al.*, 2002].

[32] Fluidized surge lobes somewhat similar to our proposed ground-hugging flows have been observed in impact experiments into viscous targets conducted by *Greeley et al.* [1980]. These surge lobes were sent by the gravitational collapse of central mound, overpassed the rim, and were emplaced. In our observation, there is no clear geomorphological evidence for such over-the-rim movement of materials that eventually formed the (inner) LESs. However, this scenario remains to be explored.

[33] The Ries impact structure in Germany appears to exhibit ejecta (Bunte Breccia) that were mobilized after the initial deposition [*Osinski*, 2004; *Osinski and Melosh*, 2004]. Interestingly, it has been noted that the Bunte Breccia at the Ries impact structure has two main components: primary ejecta excavated from the initial crater and secondary ejecta that may have incorporated underlying volatile-rich sediments [*Hörz et al.*, 1983]. These two components may correspond to the ballistically emplaced materials and the water-involved ground-hugging materials in our hypothesis. Alternatively, the Ries impact structure surficial suevites that was formed over the Bunte Breccia and was apparently

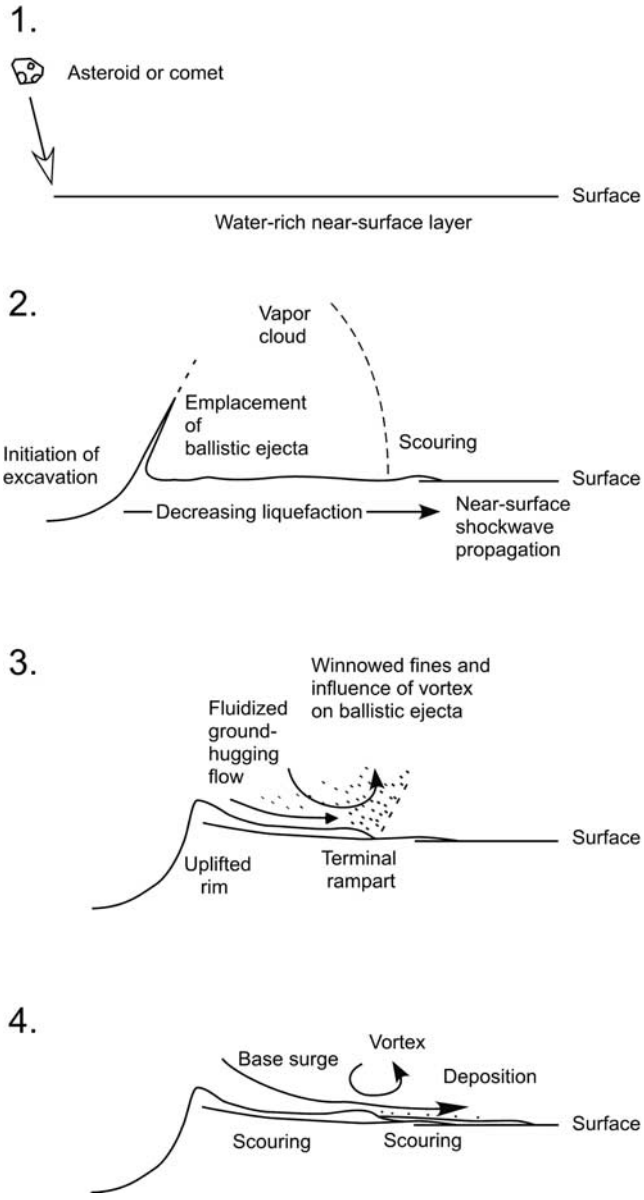

Figure 14. Schematic diagrams showing various hypothesized mechanisms of LES formation. Time progresses from 1 to 4. It is uncertain if all cases of LES formation involved all of the processes shown here. These diagrams are not to scale.

emplaced as surface flows [*Osinski and Melosh*, 2004] may be a terrestrial analogue for the ground-hugging materials.

5.2. Formation Mechanisms of Outer-Layered Ejecta Structures

[34] How about the thinner outer LESs observed with the DLE type? The majority of LES impact craters are classified to be of the single-lobate (SLE) type [e.g., *Barlow and Bradley*, 1990]. However, one detailed study on a group of the most pristine rampart craters found that the DLE type is the majority [*Demura and Kurita*, 1999]. Although intermediate morphology exists between various types of LESs as noted earlier, the distinction between thicker inner LES and thinner outer LES could be very clear in some occasions (e.g., Figures 7, 9a, 10, and 11). Therefore we think that the emplacement mechanisms of these two LES types could have been fundamentally different from each other, and both the LES types must have resulted from primary formation processes (i.e., not from secondary modification processes). Our observations indicate that the outer LESs can also have terminal rampart morphology (Figures 2c, 7c, 8a, and 8b), although the thin nature of the outer LESs makes it difficult to confirm the presence of a terminal rampart for all the cases. The outer LESs can have lower thermal inertia compared with the inner LESs as noted by *Baratoux et al.* [2005], and this situation is observation also in our study (Figure 11). This difference may be due to postimpact modification as discussed by Baratoux et al., but it may reflect ejecta-emplacement processes. The formation of the outer LESs should have occurred either before the emplacement of the thicker inner LESs, as indicated in Figure 8b, or after, as indicated in Figure 6. It is also possible that the outer LESs are made of materials formed both before and after the formation of the inner LESs.

[35] We hypothesize that the thinner outer LESs were formed by various combinations of primarily three processes (Figure 14): (1) liquefaction of water-rich near-surface sediments, (2) emplacement of ballistic ejecta-entraining water, and (3) strong winds (expanding vapor, vortex, base surge) related to the impact. Each of these processes could be dominant in some instances or equally important as others in other cases. The first process should occur before the emplacement of the ejecta curtain, and the outer LES component explained by this process is not conventional ejecta.

[36] Liquefaction due to shockwave propagation has been observed on Earth. Earthquakes that propagate through water-saturated cohesionless sediments are known to cause liquefaction. The liquefaction during the Niigata Earthquake and the Alaska Earthquake in 1964 [e.g., *Seed and Idriss*, 1967] caused substantial building damages and produced landforms such as sand volcanoes. We also note that some synsedimentary deformation features in Utah involved liquefaction, and they have been attributed to an impact event [*Alvarez et al.*, 1998] that resulted in the formation of the Upheaval Dome, a purported impact structure [*Shoemaker and Herkenhoff*, 1984; *Kriens et al.*, 1999]. It is reasonable to assume that the impact-induced shockwave produces a significant amount of liquefaction in water-rich near-surface sediments.

[37] Volatiles in the permafrost zone on Mars tend to diffuse to the atmosphere over long geological timescales [e.g., *Clifford and Hillel*, 1983; *Fanale et al.*, 1986]. However, at higher latitudes, this process is less effective, and a large amount of volatiles may reside in the near-surface layer. On Mars, extensive liquefaction due to impact events is considered to be possible by *Clifford* [2004] and *Wang et al.* [2005] on the basis of comparisons with terrestrial earthquake-induced liquefaction. Liquefaction may occur owing to the shockwave propagating outward through the volatile-rich part of the near-surface materials during the early excavation stage (Figure 14). The liquefaction should have involved shock-induced meltwater and liquid water stored in shallow aquifers although other crustal volatiles such as CO_2 and methane may also have played some roles. Melting of ice outside the excavation zone by impact shock wave is considered to be limited [*Stewart et al.*, 2004], but there are possible factors (e.g., subsurface hydrothermal convection, potent freezing-point depressing salt compo-

nents, dehydration of hydrous salts) that could increase the availability of liquid water as we discussed before.

[38] There are probably a variety of unconsolidated sediments near the surface of Mars. Such unconsolidated sediments may constitute a loosely packed grain framework, but it suddenly collapses, and the grains become temporarily suspended in the pore water under the stress. The terminal lobe (Figure 10) could be a product of horizontal movement of such a water-sediment mixture fluid and accumulation of sediments over less-liquefied areas. The impact-induced shockwave weakens with distance from the impact site, and this should determine the maximum extent of liquefied part of an outer LES. However, other factors such as the amount of water and availability of unconsolidated near-surface materials are also important in controlling the liquefaction zone.

[39] It has been found that globally, the DLE-type impact craters exist generally at mid northern latitudes (>30°N) [*Barlow and Bradley*, 1990]. Later studies reached similar conclusions, although minor concentrations of the DLE type were noted also in the southern hemisphere (<30°S) [*Barlow*, 1994; *Barlow and Perez*, 2003; *Barlow*, 2005]. This trend can be explained in the light of our liquefaction hypothesis for some outer LES formation. These mid-latitude areas are where large amounts of near-surface water ice are expected [e.g., *Fanale*, 1976; *Clifford and Hillel*, 1983; *Fanale et al.*, 1986]. In the case of the northern hemisphere, also large amounts of unconsolidated sediments derived from the Tharsis bulge and the southern highlands may have accumulated [e.g., *Lucchitta et al.*, 1986; *Baker et al.*, 1991; *Tanaka*, 1997; *Head et al.*, 1999]. Both these two conditions are favorable for the liquefaction by shockwave propagation. In addition, increased insolation due to high obliquity [e.g., *Paige*, 2002] could enhance melting of existing water ice and/or help maintaining liquid water at mid latitudes. The general lack of the DLE type beyond 60°N [*Barlow and Bradley*, 1990] may be attributed to a probable deeper hydrosphere unreachable for small-impact events and inability of water to remain liquid during the impact cratering.

[40] There are other observations, particularly in Acidalia Planitia, which are consistent with our proposed liquefaction hypothesis. The grain sizes of the outer LES are inferred to be smaller than those of the inner LES for some DLE-type impact craters (e.g., Figure 11). This is consistent with the hypotheses that the outer LESs were formed by liquefaction of fine-grained materials, whereas the inner LESs were formed by mass flows that include larger grains derived mainly from the rim area. The undulating surfaces of the outer LESs may be explained by very strong shockwave near the impact site, causing extensive liquefaction of near-surface unconsolidated sediments. The smooth light-toned material observed with one DLE-type impact crater (Figure 9b) may be explained by the separation of liquid water from the outer LES or by in situ liquefaction, and the water's eventual freezing and/or sublimation.

[41] The origins of the small mounds occurring in Acidalia Planitia including the surroundings of the studied DLE-type impact craters (Figures 9a, 10a, 12a, and 12b) are unknown. Possible interpretations based on their morphology (dome- or cone-shaped edifices and occasional occurrence of summit craters) (Figure 12b) and relatively fine-grained surface materials (Figure 11) include: (1) pingos [e.g., *Page and Murray*, 2006] and (2) mud volcanoes and/or spring mounds [e.g., *Farrand et al.*, 2005], although the pingo hypothesis for the mounds in Acidalia Planitia may have some problems as discussed by *Farrand et al.* [2005]. Other mound morphologies such as rootless cones [e.g., *Lanagan et al.*, 2001; *Bruno et al.*, 2004] and tumuli [e.g., *Glaze et al.*, 2005] are unlikely explanations for these features because of a lack of obvious associated volcanic landforms and/or difficulty in producing fine-grained surface materials. Tuff cones remain a possibility since they do not require associated lava flows and they are composed of ash-sized particles [e.g., *Farrand et al.*, 2005]. If (1) pingo or (2) mud volcano and/or spring mound interpretations are valid, their presence indicates that a large area of Acidalia Planitia is rich in volatiles and unconsolidated fine-grained sediments. Such grounds are prone to liquefaction. This is again consistent with the high occurrence of the hypothesized liquefied outer LESs in the region. If some mounds are shock-induced liquefaction features, at least part of their formation could be linked with impact events. Indeed, we point out that even a weakened shockwave propagating far away from the impact site may still cause localized liquefaction. Some mounds and also "pancake" features (Figure 9b) observed in the vicinity of the outer LESs may be manifestations of such events. Water-escape vents have been observed at the detonation sites of large TNT charges in alluvium [*Jones*, 1977] and also in an impact experiment into a water-saturated sandy target [*Ormö et al.*, 2006], and a similar process may have occurred also on Mars. At least within the areas of our investigation, there is no statistically proven increased correlation of their spatial occurrence with respect to any specific DLE-type impact craters. However, for one example of the DLE type, there is an observed indication of a continuum of processes responsible for both the outer LES and the mounds (Figure 9a).

[42] We think that the outer LESs also resulted at least partially from the ballistic emplacement of ejecta-entraining water. This is suggested by the fragmented appearance of some outer LESs (e.g., Figure 12a). *Gault and Greeley* [1978], in their impact experiments into mud targets, showed that the ejecta plume broke up into thin, irregular sheets of mud. Such broken-up fragments may land on the surface separately from the main ejecta. As pointed out by *Greeley et al.* [1980], detached ejecta deposits are observed around some Martian LES impact craters, and it is consistent also with our observation in Acidalia Planitia.

[43] The atmosphere-ejecta curtain interaction [*Schultz and Gault*, 1979; *Schultz*, 1992; *Barnouin-Jha and Schultz*, 1996; *Barnouin-Jha*, 1998] is one of the candidate processes responsible for the formation of the striations visible on inner and outer LES surfaces. We view that the resulting turbulent vortex flow could have capacity to scour the LES surfaces. If it is the case, such turbulent flow probably scoured the surfaces of the inner LESs and also of the outer LESs, contributing to some outer LES formation (Figures 6, 7d, 14). The liquefied/fluidized surfaces of both the inner and outer LESs would be particularly susceptible to such scouring, enhancing formation of the observed striations. This process may have caused deposition of fine-grained materials from the ejecta curtain and also from the eroded inner LESs, forming some outer LESs. Flow separation could be also important in the deposition of the outer LESs as suggested in

the model by *Schultz* [1992] and *Barnouin-Jha et al.* [1999a, 1999b].

[44] Besides the mechanism discussed above, two other processes of scouring for the striation formation can be envisaged. First, impact-generated vapor expanding in advance of the ejecta curtain (Figure 14) could have scoured the LES surface with supersonic winds [*Schultz*, 1992]. This type of winds can be effective in scouring the liquefied surface of the outer LES in our model. Second, a base-surge model proposed by *Boyce and Mouginis-Mark* [2006] to explain the radial scouring involves collapsing of a vertical explosion column of ejected particles and gas. The resulting turbulent, high-velocity clouds sweep outward from the crater, passing over both surfaces of the inner LES and also of the outer LES (Figure 14). Such turbulent winds may be capable of substantial erosion and consequent deposition, possibly contributing to the emplacement of the outer LES. This process could be enhanced by liquefied/fluidized surfaces of both the inner and outer LESs.

[45] The materials scoured by the vortex and the base surge from the inner LES surface should be composed of relatively fine-grained particles. And these high-velocity flows should have carried fine-grained particles derived also from the excavation cavity. Thus these fine-grained materials likely constitute at least parts of the outer LESs, whereas the inner LES surfaces are stripped of their fine-grained materials. This is consistent with the inferred smaller grain sizes (Figure 11) of the outer LES surfaces compared with those of the inner LES surfaces.

[46] The fallout suevites at the Ries impact structure was suggested to have landed on top of Bunte Breccia after winds of high velocities smoothed the breccia surface [*Von Engelhardt*, 1990]. Therefore this smoothing process and the suevites may represent terrestrial analogues for the scouring of LES surfaces and some outer LES materials, respectively.

6. Conclusions

[47] We utilized HRSC and THEMIS data sets together with MOC and MOLA data to study layered ejecta structures (LESs) of relatively pristine Martian impact craters. The morphology and morphometric properties of the LESs are extremely wide, and LES formation requires combinations of various impact processes. Ballistic ejecta emplacement should have been important to the LES formation. However, many (inner) LESs do not have topographic profiles expected from simple ballistic emplacement. Such profiles include ones that are plateau-shaped or thickening outward. The morphology of the studied (inner) LESs including the ground-hugging flows implies fluidization in their emplacement. And we hypothesize that fluidization occurred in the water-rich ballistic ejecta and structurally uplifted rim materials. The materials flowed outward owing to the momentum given by the impact, but gravity due to the height of the rim probably assisted their movement. The fluidized flows, together with ballistic emplacement and vortex produced by the atmosphere-ejecta curtain interaction, were probably essential to the (inner) LES formation.

[48] Some thinner outer LESs may have resulted from liquefaction of water-rich near-surface sediments, which should have occurred in the early phase of impact cratering. Ballistic emplacement of ejecta-entraining water may explain some detached outer LES morphology. We consider that strong winds (expanding vapor, vortex, and base surge) related to the impact produced striations scoured on both the inner and outer LESs and also contributed to the emplacement of the outer LES materials.

[49] We stress that the extremely wide-ranged LES morphology associated with Martian impact craters can be explained only with various combinations of processes. The contribution of each proposed LES formation mechanism should have been variable depending on the condition of the impact. But our proposed hypotheses may not fully explain origins of all the Martian LESs, many of which have not been studied within our limited study samples. Furthermore, effects of other parameters such as lithology (e.g., layered targets not only of various rock types but also with varying concentrations of volatiles, crystalline versus sedimentary), diverse atmospheric conditions (e.g., pressure, compositions), clathrate decomposition, and crustal volatiles other than water (e.g., CO_2, methane) may have significant influences on the LES emplacement, but their effects are not explored in our working hypotheses. We plan to examine these parameters in the future.

[50] Testing of the proposed hypotheses for the formation of the LESs could be achieved by combining more detailed geomorphologic/geomorphic investigations, numerical simulations, laboratory experiments, and terrestrial analogue studies.

[51] **Acknowledgments.** We thank the HRSC Experiment Teams at DLR Berlin and Freie Universitaet Berlin as well as the Mars Express Project Teams at ESTEC and ESOC for their successful planning and acquisition of data as well as for making the processed data available to the HRSC Team. We acknowledge the effort of the HRSC Co-Investigator Team members and their associates who have contributed to this investigation in the preparatory phase and in scientific discussions within the Team. The comments and suggestions by David Baratoux and Ron Greeley were particularly valuable. We thank Hirohide Demura and Jens Ormö for constructive discussions on formation processes of LESs. Sarah Stewart and Steve Baloga provided review comments that greatly improved the manuscript. This project was supported by the Mars Express Geographic Information System (MEGIS) program. The research was financed by the Italian Space Agency.

References

Albertz, J., et al. (2005), HRSC on Mars Express—Photogrammetric and cartographic research, *Photogramm. Eng. Remote Sens.*, *71*, 1153–1166.

Allen, P. A. (1997), *Earth Surface Processes*, 404 pp., Blackwell Sci., Malden, Mass.

Alvarez, W., E. Staley, D. O'Connor, and M. A. Chan (1998), Synsedimentary deformation in the Jurassic of southeastern Utah—A case of impact shaking?, *Geology*, *26*(7), 579–582.

Baker, V. R., R. G. Strom, V. C. Gulick, J. S. Kargel, G. Komatsu, and V. S. Kale (1991), Ancient oceans and ice sheets and the hydrological cycle on Mars, *Nature*, *352*, 589–594.

Baloga, S. M., S. A. Fagents, and P. J. Mouginis-Mark (2005), Emplacement of Martian rampart crater deposits, *J. Geophys. Res.*, *110*, E10001, doi:10.1029/2004JE002338.

Baratoux, D., C. Delacourt, and P. Allemand (2002), An instability mechanism in the formation of the Martian lobate craters and the implications for the rheology of ejecta, *Geophys. Res. Lett.*, *29*(8), 1210, doi:10.1029/2001GL013779.

Baratoux, D., N. Mangold, and P. Pinet (2005), Thermal properties of lobate ejecta in Syrtis Major, Mars: Implications for the mechanisms of formations, *J. Geophys. Res.*, *110*, E04011, doi:10.1029/2004JE002314.

Barlow, N. G. (1994), Sinuosity of Martian rampart ejecta deposits, *J. Geophys. Res.*, *99*(E5), 10,927–10,935.

Barlow, N. G. (2005), A review of Martian impact crater ejecta structures and their implications for target properties, in *Large Meteorite Impacts III*, edited by T. Kenkmann, F. Hörz, and A. Deutsch, *Geological Society of America Special Paper*, *384*, pp. 433–442.

Barlow, N. G., and T. L. Bradley (1990), Martian impact craters: Correlations of ejecta and interior morphologies with diameter, latitude, and terrain, *Icarus*, *87*, 156–179.

Barlow, N. G., and C. B. Perez (2003), Martian impact crater ejecta morphologies as indicators of the distribution of subsurface volatiles, *J. Geophys. Res.*, *108*(E8), 5085, doi:10.1029/2002JE002036.

Barlow, N. G., J. M. Boyce, F. M. Costard, R. A. Craddock, J. B. Garvin, S. E. H. Sakimoto, R. O. Kuzmin, D. J. Roddy, and L. A. Soderblom (2000), Standardizing the nomenclature of Martian impact crater ejecta morphologies, *J. Geophys. Res.*, *105*, 26,733–26,738.

Barlow, N. G., J. Koroshetz, and J. M. Dohm (2001), Variations in the onset diameter for Martian layered ejecta morphologies and their implications for subsurface volatile reservoirs, *Geophys. Res. Lett.*, *28*, 3095–3098.

Barnouin-Jha, O. S. (1998), Lobateness of impact ejecta deposits from atmospheric interactions, *J. Geophys. Res.*, *103*(E11), 25,739–25,756.

Barnouin-Jha, O. S., and P. H. Schultz (1996), Ejecta entrainment by impact-generated ring vortices: Theory and experiments, *J. Geophys. Res.*, *101*(E9), 21,099–21,115.

Barnouin-Jha, O. S., P. H. Schultz, and J. H. Lever (1999a), Investigating the interactions between an atmosphere and an ejecta curtain: 1. Wind tunnel tests, *J. Geophys. Res.*, *104*, 27,105–27,131.

Barnouin-Jha, O. S., P. H. Schultz, and J. H. Lever (1999b), Investigating the interactions between an atmosphere and an ejecta curtain: 2. Numerical experiments, *J. Geophys. Res.*, *104*, 27,117–27,131.

Barnouin-Jha, O. S., S. Baloga, and L. Glaze (2005), Comparing landslides to fluidized crater ejecta on Mars, *J. Geophys. Res.*, *110*, E04010, doi:10.1029/2003JE002214.

Betts, B., and B. Murray (1993), Thermally distinct ejecta blankets from Martian craters, *J. Geophys. Res.*, *98*(E6), 11,043–11,059.

Boyce, J. M., and P. J. Mouginis-Mark (2005), Martian craters viewed by the THEMIS Instrument: Double-layered ejecta craters, *Role of volatiles and atmospheres on Martian impact craters* [CD-ROM], abstract 3009.

Boyce, J. M., and P. J. Mouginis-Mark (2006), Martian craters viewed by the THEMIS instrument: Double-layered ejecta craters, *J. Geophys. Res.*, *111*, E10005, doi:10.1029/2005JE002638.

Bruno, B. C., S. A. Fagents, T. Thordarson, S. M. Baloga, and E. Pilger (2004), Clustering within rootless cone groups on Iceland and Mars: Effect of nonrandom processes, *J. Geophys. Res.*, *109*, E07009, doi:10.1029/2004JE002273.

Carr, M. H., L. S. Crumpler, J. A. Cutts, R. Greeley, J. E. Guest, and H. Masursky (1977), Martian impact craters and the emplacement of ejecta by surface flow, *J. Geophys. Res.*, *82*, 4055–4065.

Cave, J. A. (1993), Ice in the northern lowlands and southern highlands of Mars and its enrichment beneath the Elysium lavas, *J. Geophys. Res.*, *98*(E6), 11,079–11,097.

Clifford, S. M. (2003), The limits of theoretical modeling and geomorphic interpretation in assessing the present distribution of subsurface H_2O on Mars, *Lunar Planet. Sci.* [CD-ROM], *XXXIV*, abstract 2118.

Clifford, S. M. (2004), The early climate of Mars: Warm, cold or forever unknowable? Ambiguities resulting from impact seismicity and hydrothermal activity, in *2nd Conf. on Early Mars*, abstract 8076.

Clifford, S. M., and D. Hillel (1983), The stability of ground ice in the equatorial region of Mars, *J. Geophys. Res.*, *88*, 2456–2474.

Costard, F. M. (1989), Asymmetric distribution of volatiles on Mars, *Lunar Planet. Sci.*, *XX*, 187–188.

Costard, F. M., and J. S. Kargel (1995), Outwash plains and thermokarst on Mars, *Icarus*, *114*, 93–112.

Demura, H., and K. Kurita (1998), A shallow volatile layer at Chryse Planitia, Mars, *Earth Planets Space*, *50*, 423–429.

Demura, H. and K. Kurita (1999), Formation of fluidized craters on Mars, *Lunar Planet. Sci.* [CD-ROM], *XXX*, abstract 1630.

Fanale, F. P. (1976), Martian volatiles: Their degassing history and geochemical fate, *Icarus*, *28*, 179–202.

Fanale, F. P., J. R. Salvail, A. P. Zentand, and S. E. Postawko (1986), Global distribution and migration of subsurface ice on Mars, *Icarus*, *67*, 1–18.

Farrand, W. H., L. R. Gaddis, and L. Keszthelyi (2005), Pitted cones and domes on Mars: Observations in Acidalia Planitia and Cydonia Mensae using MOC, THEMIS, and TES data, *J. Geophys. Res.*, *110*, E05005, doi:10.1029/2004JE002297.

Garvin, J. B., and J. J. Frawley (1998), Geometric properties of Martian impact craters: Preliminary results from the Mars Orbiter Laser Altimeter, *Geophys. Res. Lett.*, *25*(24), 4405–4408.

Garvin, J. B., S. E. Sakimoto, J. J. Frawley, and C. Schnetzler (2000), North polar region craterforms on Mars: Geometric characteristics from the Mars Orbiter Laser Altimeter, *Icarus*, *144*, 329–352.

Gault, D. E., and R. Greeley (1978), Exploratory experiments of impact craters formed in viscous targets: Analogs for Martian rampart craters, *Icarus*, *34*, 486–495.

Glaze, L. S., S. W. Anderson, E. R. Stofan, S. Baloga, and S. E. Smrekar (2005), Statistical distribution of tumuli on pahoehoe flow surfaces: Analysis of examples in Hawaii and Iceland and potential applications to lava flows on Mars, *J. Geophys. Res.*, *110*, B08202, doi:10.1029/2004JB003564.

Greeley, R., J. H. Fink, D. E. Gault, D. B. Snyder, J. E. Guest, and P. H. Schultz (1980), Impact cratering in viscous targets: Experimental results, *Proc. Lunar Planet. Sci. Conf.*, *11*, 2075–2097.

Hauber, E., and G. Neukum (2004), Mars as never seen before, *Astron. Geophys.*, *45*, 2.21–2.27.

Head, J. W., and R. Roth (1976), Mars pedestal craters escarpments: Evidence for ejecta-related emplacement, in *Symposium of Planetary Cratering Mechanics*, pp. 50–52, Lunar and Planet. Inst., Houston, Tex.

Head, J. W., H. Hiesinger, M. A. Ivanov, M. A. Kreslavsky, S. Pratt, and B. J. Thomson (1999), Possible oceans in Mars: Evidence from Mars Orbiter Laser Altimeter data, *Science*, *286*, 2134–2137.

Hörz, F., R. Ostertag, and D. A. Rainey (1983), Bunte breccia of the Ries: Continuous deposits of large impact craters, *Rev. Geophys. Space Phys.*, *21*, 1667–1725.

Ivanov, B. A. (1996), Spread of ejecta from impact craters and the possibility of estimating the volatile content of the Martian crust, *Sol. Syst. Res.*, *30*(1), 36–50.

Ivanov, B., and A. Pogoretsky (1996), Bingham parameters for fluidized ejecta spreading on Mars and Martian volatiles, *Lunar Planet. Sci.*, *XXVII*, 587–588.

Jones, G. H. S. (1977), Complex craters in alluvium, In: *Impact and Explosion Cratering*, edited by D. J. Roddy, R. O. Pepin, and R. B. Merril, pp. 163–183, Pergamon Press New York.

Kargel, J. S. (1986), Morphologic variations of Martian rampart craters and their dependencies and implications, *Lunar Planet. Sci.*, *XVII*, 410–411.

Kargel, J. S., and G. M. Marion (2004), Mars as a salt-, acid-, and gas-hydrate world, *Lunar Planet. Sci.* [CD-ROM], *XXXV*, abstract 1965.

Kriens, B. J., E. M. Shoemaker, and K. E. Herkenhoff (1999), Geology of the Upheaval Dome impact structure, southeast Utah, *J. Geophys. Res.*, *104*, 18,867–18,887.

Kuzmin, R. O., N. N. Bobina, E. V. Zabalueva, and V. P. Shashkina (1988), Structure inhomogeneities of the Martian cryolithosphere, *Sol. Syst. Res.*, *22*, 195–212.

Lanagan, P. D., A. S. McEwen, L. P. Keszthelyi, and T. Thordarson (2001), Rootless cones on Mars indicating the presence of shallow equatorial ground ice in recent times, *Geophys. Res. Lett.*, *28*, 2365–2368.

Lucchitta, B. K. (1987), Valles Marineris, Mars: Wet debris flows and ground ice, *Icarus*, *72*, 411–429.

Lucchitta, B. K., H. M. Ferguson, and C. Summers (1986), Sedimentary deposits in the northern lowland plains, Mars, *J. Geophys. Res.*, *91*, 166–174.

McCauley, J. F. (1973), Mariner 9 evidence for wind erosion in the equatorial and mid-latitude regions of Mars, *J. Geophys. Res.*, *78*, 4123–4137.

McGetchin, T. R., M. Settle, and J. W. Head (1973), Radial thickness variation in impact crater ejecta: Implications for lunar basin deposits, *Earth Planet. Sci. Lett.*, *20*, 226–236.

Melosh, H. J. (1989), *Impact Cratering*, 245 pp., Oxford Univ. Press, New York.

Montgomery, D. R., and A. Gillespie (2005), Formation of Martian outflow channels by catastrophic dewatering of evaporite deposits, *Geology*, *33*, 625–628.

Moore, H. J., C. A. Hodges, and D. H. Scott (1974), Multi-ringed basins—Illustrated by Orientale and associated features, *Proc. Lunar Planet. Sci. Conf. 5th*, pp. 71–100.

Mouginis-Mark, P. J. (1979), Martian fluidized crater morphology: Variations with crater size, latitude, altitude and target material, *J. Geophys. Res.*, *84*, 8011–8022.

Mouginis-Mark, P. J. (1981), Ejecta emplacement and modes of formation of Martian fluidized ejecta craters, *Icarus*, *45*, 60–76.

Mouginis-Mark, P. J., and S. M. Baloga (2006), Morphology and geometry of the distal ramparts of Martian impact craters, *Meteorit. Planet. Sci.*, *41*, 1469–1482.

Mouginis-Mark, P. J., and J. M. Boyce (2005), The unique attributes of Martian double layered ejecta craters, *Lunar Planet. Sci.* [CD-ROM], *XXXVI*, abstract 1111.

Mouginis-Mark, P. J., H. Garbeil, J. M. Boyce, C. S. E. Ui, and S. M. Baloga (2004), The geometry of Martian impact craters: First results from an interactive software package, *J. Geophys. Res.*, *109*, EO8006, doi:10.1029/2003JE002147.

Oberst, J., et al. (2004), The mapping performance of the HRSC/SRC in Mars orbit, *ISPRS Congress*, *XX*, available at http://www.isprs.org/istanbul2004/comm4/papers/546.pdf.

Ormö, J., M. Lindström, A. Lepinette, J. Martinez-Frias, and E. Diaz-Martinez (2006), Cratering and modification of wet-target craters: Projectile impact

experiments and field observations of the Lockne marine-target crater (Sweden), *Meteorit. Planet. Sci.*, *41*, 1605–1612.
Osinski, G. R. (2004), Impact melt rocks from the Ries impact structure, Germany: An origin as impact melt flows?, *Earth Planet. Sci. Lett.*, *226*, 529–543.
Osinski, G. R. (2006), Role of volatiles in the emplacement of ejecta deposits around Martian impact craters, *Lunar Planet. Sci.* [CD-ROM], *XXXVII*, abstract 1060.
Osinski, G. R., and H. J. Melosh (2004), A search for terrestrial analogues to Martian layered ejecta structures, *Mars crater consortium meeting VII*, abstract 0704.
Page, D. P., and J. B. Murray (2006), Stratigraphical and morphological evidence for pingo genesis in the Cerberus plains, *Icarus*, *183*, 46–54.
Paige, D. A. (2002), Near-surface liquid water on Mars, *Lunar Planet. Sci.* [CD-ROM], *XXXIII*, abstract 2049.
Reiss, D., E. Hauber, G. Michael, R. Jaumann, G. Neukum, and the HRSC Co-Investigator Team (2005), Small rampart craters in an equatorial region on Mars: Implications for near-surface water or ice, *Geophys. Res. Lett.*, *32*, L10202, doi:10.1029/2005GL022758.
Schultz, P. H. (1992), Atmospheric effects on ejecta emplacement, *J. Geophys. Res.*, *97*, 13,257–13,302.
Schultz, P. H., and D. E. Gault (1979), Atmospheric effects on Martian ejecta emplacement, *J. Geophys. Res.*, *84*(B13), 7669–7687.
Seed, H. B., and I. M. Idriss (1967), Analysis of soil liquefaction: Niigata Earthquake, *J. Soil Mech. Found. Div., Am. Soc. Civ. Eng.*, *93*(SM3), 83–108.
Shoemaker, E. M., and K. E. Herkenhoff (1984), Upheaval dome impact structure, *Lunar Planet. Sci.*, 778–779, abstract.
Stewart, S. T., and T. J. Ahrens (2003), Shock Hugoniot of H_2O ice, *Geophys. Res. Lett.*, *30*(6), 1332, doi:10.1029/2002GL016789.
Stewart, S. T., and G. J. Valiant (2006), Martian subsurface properties and crater formation processes inferred from fresh impact crater geometries, *Meteorit. Planet. Sci.*, *41*, 1509–1537.
Stewart, S. T., T. J. Ahrens, and J. D. O'Keefe (2004), Impact-induced melting of near-surface water ice on Mars, in *Shock Compression of Condensed Matter-2003*, edited by M. D. Furnish, Y. M. Gupta, and J. W. Forbes, pp. 1484–1487, American Institute of Physics.
Strom, R. G., S. K. Croft, and N. G. Barlow (1992), The Martian impact cratering record, in *Mars*, edited by H. H. Kieffer, B. M. Jakowsky, C. Snyder, and M. Matthews, pp. 383–423, Univ. of Ariz. Press, Tucson.
Tanaka, K. L. (1997), Sedimentary history and mass flow structures of Chryse and Acidalia Planitiae, Mars, *J. Geophys. Res.*, *102*, 4131–4149.
Travis, B. J., N. D. Rosenberg, and J. N. Cuzzi (2003), On the role of widespread subsurface convection in bringing liquid water close to Mars' surface, *J. Geophys. Res.*, *108*(E4), 8040, doi:10.1029/2002JE001877.
Von Engelhardt, W. (1990), Distribution, petrography and shock metamorphism of the ejecta of the Ries crater in Germany—A review, *Tectonophysics*, *171*, 259–273.
Wang, C.-Y., M. Manga, and A. Wong (2005), Floods on Mars released from groundwater by impact, *Icarus*, *175*, 551–555.

G. Komatsu, S. Di Lorenzo, G. G. Ori, and A. P. Rossi, International Research School of Planetary Sciences, Università "G. d'Annunzio", Viale Pindaro 42, 65127, Pescara, Italy. (goro@irsps.unich.it)
G. Neukum, Institut fuer Geologische Wissenschaften, Freie Universitaet Berlin, Malteserstr. 74100, Bldg. D, 12249, Berlin, Germany.